

9-2015

On the Performance of SR and FR Protocols for OSTBC based AF-MIMO Relay System with Channel and Noise Correlations

Batu K. Chalise
Cleveland State University

Follow this and additional works at: https://engagedscholarship.csuohio.edu/enece_facpub

 Part of the [Electrical and Computer Engineering Commons](#)

[How does access to this work benefit you? Let us know!](#)

Publisher's Statement

(c) 2015 IEEE. Personal use is permitted, but republication/redistribution requires IEEE permission. See http://www.ieee.org/publications_standards/publications/rights/index.html for more information. This article has been accepted for publication in a future issue of this journal, but has not been fully edited. Content may change prior to final publication.

Original Citation

B. Chalise, "On the Performance of SR and FR Protocols for OSTBC based AF-MIMO Relay System with Channel and Noise Correlations," *Vehicular Technology, IEEE Transactions on*, 2015.

Repository Citation

Chalise, Batu K., "On the Performance of SR and FR Protocols for OSTBC based AF-MIMO Relay System with Channel and Noise Correlations" (2015). *Electrical Engineering & Computer Science Faculty Publications*. 336.
https://engagedscholarship.csuohio.edu/enece_facpub/336

This Article is brought to you for free and open access by the Electrical Engineering & Computer Science Department at EngagedScholarship@CSU. It has been accepted for inclusion in Electrical Engineering & Computer Science Faculty Publications by an authorized administrator of EngagedScholarship@CSU. For more information, please contact library.es@csuohio.edu.

On the Performance of SR and FR Protocols for OSTBC based AF-MIMO Relay System with Channel and Noise Correlations

Batu K. Chalise, *Senior Member, IEEE*

Abstract—This paper proposes selection relaying (SR) protocol for a cooperative multiple-input multiple-output (MIMO) relay system that consists of a direct link between a source and a destination. The system has only receive-side channel state information (CSI), spatially correlated MIMO channels, and the receiver nodes observe spatially correlated noise. The transmit nodes employ orthogonal space-time block codes (OSTBC), whereas the receiver nodes employ optimum minimum mean-square-error (MMSE) detection. The SR protocol, which transmits via the relay only when the direct link between the source and destination is in outage, is compared with the fixed relaying (FR) protocol which always uses the relay. By deriving novel asymptotic expressions of the outage probabilities, it is analytically shown that both protocols provide the same diversity gain. However, the coding gain (CG) of the SR protocol can be much better than that of the FR protocol. In particular, when all MIMO links have the same effective rank, irrespective of its value, the SR protocol provides better CG than the FR scheme if the target information rate is greater than $\ln_2(3)$ bits per channel use. Simulation results support theoretical analysis and show that the SR scheme can significantly outperform FR method, which may justify the increased complexity due to one-bit feedback requirement in the SR protocol.

Index Terms—MIMO relay, channel state information, OSTBC, selection and fixed relaying, outage probability, MMSE receivers

I. INTRODUCTION

In recent years, cooperative communications with both single-antenna and multiple-input multiple-output (MIMO) relays have garnered significant interests [1]-[4]. Cooperative relays are also expected to be a part of heterogeneous networks in fifth generation communication systems [5]. By employing precoding and decoding techniques, cooperative systems with MIMO nodes provide both spatial multiplexing and diversity gains. However, precoding requires a transmitter to have channel state information (CSI) which is generally obtained via feedback from the receiver. In order to minimize the cost of CSI feedback and simplify the system design without compromising with the system diversity gain, the transmitter often employs orthogonal space-time block codes (OSTBC) [6]-[8]. Because of the optimal decoding at low complexity and the promising diversity gains, OSTBC based designs are also deployed in LTE systems, where full-rate OSTBCs,

namely the Alamouti codes are employed in frequency domain for the transmitters with two and four antennas [9].

The OSTBC-based dual-hop *non-coherent* amplify-and-forward (AF) MIMO relay system is proposed in [10] and [11] for Rayleigh and Ricean fading channels, respectively. In both papers, source employs OSTBC encoding and the relay does not have receive-side CSI. On the other hand, performance analysis of the OSTBC-based dual-hop *coherent* AF relay system is proposed for Nakagami- m correlated channels in [12] and [13], where single-antenna and multi-antenna relay are considered, respectively. In [13], both source and relay nodes use OSTBC, whereas direct link between the source and destination is not considered in [10]-[13]. The closed-form expression of the exact outage probability and the corresponding asymptotic expression are derived in [14] for a coherent MIMO relay system that uses decode-and-forward relay protocol, OSTBCs at the source and relay nodes, and has the direct link. In [15], the performance of the OSTBC-based coherent AF MIMO relay network is analyzed, in which the relays estimate the source signal and forward it to the destination without decoding. This work is extended in [16] to MIMO channels with spatial correlation and the direct link with the keyhole effect. The works in [14]-[16] consider a fixed relaying (FR) scheme where the relay is always employed and the system follows a two-phase transmission, i.e., in the first phase the source transmits and in the second phase the relay transmits. Moreover, noise at both the relay and destination nodes are spatially uncorrelated.

In practice, spatial channel correlations and coupling among receiver antennas can make the received signal and noise to become correlated [17]-[18]. Many prior works have analyzed the effects of correlated noise (and colored interference) on the system design and performance for different applications. In [19], the authors determine the MIMO channel capacity in the presence of correlated noise, whereas in [20], coordinated beamforming technique is proposed for a broadcast channel with signal and noise correlation at the receiver, where correlation occurs in the presence of receiver mutual coupling. The optimum design of relay processing coefficients is proposed in [21] for an AF relay system where the noise among distributed single-antenna relays is assumed to be correlated, for example, due to common interference observed by the relays. In [22], the effects of spatial channel correlation, antenna coupling, superdirectivity and noise correlation are taken into account while designing the AF-MIMO relay for a system with multiple single-antenna sources and a multi-

Copyright (c) 2015 IEEE. Personal use of this material is permitted. However, permission to use this material for any other purposes must be obtained from the IEEE by sending a request to pubs-permissions@ieee.org.

The author is with the Department of Electrical Engineering and Computer Science, Cleveland State University, 2121 Euclid Avenue, OH 44115, USA (email: b.chalise@csuohio.edu).

antenna destination. As in [10]-[16], both designs, [21] and [22], consider the FR protocol.

However, in the presence of the direct link between the source and destination, it is known from [23] that selection relaying (SR) for the AF relay system simplifies the joint design of the beamformers and performs better than the joint beamformer design based on FR protocol. In the SR approach, the AF relay is used only if the direct link fails to support the targeted information rate. Moreover, the source changes the modulation order in a way that the effective rate of information transmission via the relay remains same as that corresponding to the direct link. Motivated from [23]¹, we propose SR protocol for an OSTBC-based cooperative coherent MIMO relay system that has a direct link, only receive-side CSI, and is subject to spatially correlated channels and noise. According to our best source of knowledge, neither such a system has been investigated nor the FR and SR protocols have been analytically compared in terms of diversity and coding gains (CG)².

In this paper, we consider a cooperative MIMO relay system where the relay and destination nodes observe spatially correlated noise and the MIMO channels are subject to spatial correlation³. The source encodes its signal using OSTBC. The relay employs a general linear receiver such as the minimum mean-square error (MMSE) receiver to estimate the source signal and forwards the resulting signal to the destination after OSTBC encoding. The destination also uses MMSE receiver to estimate and decode the source signal, received via the source-destination (S-D) and the two hop source-relay-destination (S-R-D) links. The orthogonality property of OSTBC is exploited to obtain the symbol estimates, and the signal-to-noise ratios (SNRs) corresponding to the S-D and S-R-D links.

Using a single-bit feedback from the destination, the SR protocol employs MIMO relay only if the S-D link is in *outage* which is defined as an instant in which the supported information rate is below the rate targeted by the source. Since it is difficult to obtain sufficient insights from the exact outage probability expressions, novel asymptotic expressions are derived to obtain the coding and diversity gains of the SR and FR protocols. It is shown that the performance depends not only on the transmit and receive-side channel correlation

¹Although the SR protocol for the AF MIMO relay system, to the best of our knowledge, was first proposed in [23] as an improved alternative approach to the FR protocol, there are two vital differences between [23] and this paper. First, the system models of [23] and this paper are completely different. In particular, [23] considers the relay system where MIMO channels and noise at receive nodes are spatially uncorrelated, and transmit-receive beamforming is employed, i.e., the knowledge of transmit-side CSI is also available. Second, [23] lacks a theoretical analysis for explaining the performance gains of the SR protocol over the FR protocol, which in fact were only evident from simulation results therein.

²It should be emphasized that the proposed analysis can also be extended to correlated Nakagami- m fading channels. In such a case, the resulting exact and approximated outage probability expressions for the SR and FR protocols, respectively, appear to be much more complicated than those in correlated Rayleigh fading channels. As such, neither a comprehensive asymptotic comparison between two methods can be proposed with sufficient conciseness nor such comparison provides important insights on their relative performance difference. Therefore, we keep our proposed analysis to correlated Rayleigh fading case.

³The modeling and calculation of noise and channel correlation matrices depend on underlying physical phenomena [17]-[22].

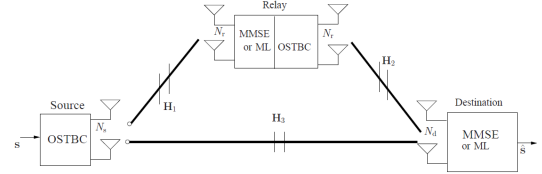


Fig. 1. OSTBC based MIMO relay system

matrices but also on the covariance matrices of noise at the receiver nodes. Although both protocols achieve the same diversity, the CG of the SR protocol can be much better than that of the FR protocol, especially for larger values of target information. In particular, when all MIMO links have the same *effective rank*⁴, irrespective of its exact value, the SR protocol provides better CG than the FR protocol for the target rates greater than $\ln_2(3)$ bits per channel use (b.p.c.u). This performance improvement may justify the latter's increased complexity due to one-bit feedback requirement.

The remainder of this paper is organized as follows. The system model and relaying protocols are described in Section II. The SNRs for the direct and dual-hop links are derived in Section III. In Section IV, performance analysis of the SR and FR protocols is presented along with the derivations for the diversity gains. The CGs of the two protocols are compared in Section V. Simulation results are presented in Section VI and conclusions are drawn in Section VII. *Notations*: Upper (lower) bold face letters will be used for matrices (vectors); $(\cdot)^T$, $(\cdot)^H$, $E\{\cdot\}$, \mathbf{I}_n and $\text{diag}(\mathbf{x})$ denote the transpose, Hermitian transpose, mathematical expectation, $n \times n$ identity matrix and the diagonal matrix formed from \mathbf{x} , respectively. $\mathcal{R}(\cdot)$, $\mathcal{I}(\cdot)$, $\text{vec}(\mathbf{X})$, $\text{tr}(\cdot)$, $\mathcal{C}/\mathcal{R}^{M \times M}$, \otimes , and $([\mathbf{X}]_{k,:})$ denote the real part, imaginary part, vectorized form of the matrix \mathbf{X} , matrix trace operator, space of $M \times M$ matrices with complex/real entries, the Kronecker product, and the k th row of the matrix \mathbf{X} , respectively. The following relations for matrix operations are often used in this paper [24].

$$\text{Re}(\mathbf{A}\mathbf{B}) = [\text{Re}(\mathbf{A}), -\text{Im}(\mathbf{A})][\text{Re}(\mathbf{B})^T, \text{Im}(\mathbf{B})^T]^T \quad (1a)$$

$$\text{Im}(\mathbf{A}\mathbf{B}) = [\text{Im}(\mathbf{A}), \text{Re}(\mathbf{A})][\text{Re}(\mathbf{B})^T, \text{Im}(\mathbf{B})^T]^T \quad (1b)$$

$$\text{tr}(\mathbf{A}^T \mathbf{B}) = \text{vec}(\mathbf{A})^T \text{vec}(\mathbf{B}) \quad (1c)$$

$$\text{vec}(\mathbf{A}\mathbf{X}\mathbf{B}) = (\mathbf{B}^T \otimes \mathbf{A})\text{vec}(\mathbf{X}) \quad (1d)$$

$$(\mathbf{A} \otimes \mathbf{B})(\mathbf{C} \otimes \mathbf{D}) = (\mathbf{A}\mathbf{C} \otimes \mathbf{B}\mathbf{D}) \quad (1e)$$

II. SYSTEM MODEL AND RELAYING PROTOCOLS

We consider a cooperative MIMO relay system where a source, a relay and a destination are respectively equipped with N_s , N_r and N_d antennas. The block diagram of the system is shown in Fig. 1. The source and relay do not have transmit-side CSI. The source-relay (S-R), relay-destination (R-D) and S-D MIMO channels are assumed to be flat fading spatially correlated Rayleigh channels. The relay is a coherent AF relay, operates in a half-duplex mode and follows either the standard

⁴The effective rank is the function of channel as well as noise correlation matrices.

FR protocol or the SR protocol.

The source node broadcasts OSTBC encoded signal. Let r_t b.p.c.u be the information rate targeted by the source. More specifically, suppose that the source transmits a vector of complex symbols drawn from a constellation \mathcal{Q}_m , where m stands for the modulation order. Let N_b be the number of bits transmitted by the source in T channel uses. In the SR protocol, the destination node broadcasts one-bit feedback signal to indicate whether it is in outage. If the feedback bit is a non-acknowledgment, i.e., an indication for the outage, the source broadcasts its signal with the same target rate of r_t b.p.c.u. Because the relay is half-duplex, the source requires to transmit more bits to maintain the same target rate. We propose that the source transmits symbols from higher-order constellation, i.e., $2N_b$ bits from the constellation \mathcal{Q}_{2m} . The relay estimates the source signal with a linear MMSE receiver, encodes the estimated symbols with the OSTBC and transmits the resulting signals to the destination. Thus, $2N_b$ bits transmitted via the S-R-D channel occupy $2T$ channel uses. The destination employs MMSE receiver to decode the signals received from the relay. On the other hand, if the feedback bit is an acknowledgment, indicating that there is no outage, the source transmits at the rate r_t (N_b bits in T channel uses) using the S-D link. In the SR protocol, the destination is said to be in outage when transmissions via both the S-R-D and S-D links fail⁵.

In the FR protocol, during the first transmission phase, the source transmits, whereas the relay and destination receive the signal. In the second transmission phase, the relay transmits and the destination combines signals received from the source and relay. In order to make a fair comparison, we use the same target rate as in the SR protocol (i.e., r_t) to define the outage at the destination. Because the end-to-end transmission from the source to the destination always occupies $2T$ channel uses in the FR protocol, the source transmits data using the constellation \mathcal{Q}_{2m} to maintain the rate r_t .

III. SIGNAL MODEL AND PROPOSED SCHEME

The signals received by the relay and the destination are, respectively, given by

$$\begin{aligned} \mathbf{Y}_1 &= \sqrt{\frac{P_s \mu_1}{N_s}} \tilde{\mathbf{H}}_1 \mathbf{S} + \mathbf{V}_1 \rightarrow \mathbf{Y}_1 = \mathbf{H}_1 \mathbf{S} + \mathbf{V}_1 \\ \mathbf{Y}_3 &= \sqrt{\frac{P_s \mu_3}{N_s}} \tilde{\mathbf{H}}_3 \mathbf{S} + \mathbf{V}_3 \rightarrow \mathbf{Y}_3 = \mathbf{H}_3 \mathbf{S} + \mathbf{V}_3 \end{aligned} \quad (2)$$

where $\tilde{\mathbf{H}}_1 \in \mathcal{C}^{N_r \times N_s}$ and $\tilde{\mathbf{H}}_3 \in \mathcal{C}^{N_d \times N_s}$ are the normalized S-R and S-D MIMO channels, μ_1 and μ_2 are the corresponding path gains, and P_s is the transmit power of the source node. $\mathbf{V}_1 \in \mathcal{C}^{N_r \times T}$, $\mathbf{V}_3 \in \mathcal{C}^{N_d \times T}$ are due to additive Gaussian noise, where each column of the matrices is a N_r/N_d column vector with correlated complex Gaussian random variables. $\mathbf{S} \in \mathcal{C}^{N_s \times T}$ is the OSTBC formed from a set of K complex symbols $\mathcal{S} = [s_1, s_2, \dots, s_K]$, where $\mathbb{E}\{|s_k|^2\} = 1$, $\forall k$ and T is the number of channel uses during which the channels remain constant (also the time dimension of the OSTBC). The

⁵We consider that when the destination is not in outage, it can correctly decode the source symbol.

path gains μ_1 and μ_3 are given by $\mu_1 = d_1^{-\zeta}$ and $\mu_3 = d_3^{-\zeta}$, where d_1 and d_3 are respectively the S-R and S-D distances, and ζ is the path-loss exponent. Note that we consider that the destination and relay nodes move within a limited geographical area where big obstacles do not exist. As such, the effect of shadow fading is negligible and the outage in this paper is mainly due to small-scale fading.⁶ The OSTBC matrix \mathbf{S} satisfies $\mathbf{S}^H \mathbf{S} = \|\mathbf{s}\|^2 \mathbf{I}_K$ where the entries of \mathbf{S} consist of linear combinations of $\{s_k\}_{k=1}^K$ as

$$\mathbf{S} = \sum_{k=1}^K \mathbf{C}_k \mathcal{R}(s_k) + \mathbf{D}_k \mathcal{I}(s_k), \quad (3)$$

and \mathbf{C}_k and \mathbf{D}_k are the dispersion matrices. Note that $\mathbf{C}_k = \mathbf{S}(\mathbf{e}_k)$ and $\mathbf{D}_k = \mathbf{S}(\mathbf{j}\mathbf{e}_k)$, where \mathbf{e}_k is a vector of ones and zeros with one at the k th symbol in \mathbf{S} . For an example, in the case of Alamouti code, we have $\mathbf{C}_1 = \begin{bmatrix} 1 & 0 \\ 0 & 1 \end{bmatrix}$, $\mathbf{C}_2 = \begin{bmatrix} 0 & 1 \\ -1 & 0 \end{bmatrix}$, $\mathbf{D}_1 = \begin{bmatrix} \mathbf{j} & 0 \\ -\mathbf{j} & 0 \end{bmatrix}$ and $\mathbf{D}_2 = \begin{bmatrix} 0 & \mathbf{j} \\ \mathbf{j} & 0 \end{bmatrix}$. The received signal \mathbf{Y}_1 is expressed in vector form as

$$\mathbf{y}_1 = \mathbf{H}_{e,1} \tilde{\mathbf{s}} + \mathbf{v}_1, \quad \text{where} \quad (4)$$

$$\begin{aligned} \mathbf{y}_1 &= \begin{bmatrix} \text{vec}(\mathcal{R}(\mathbf{Y}_1)) \\ \text{vec}(\mathcal{I}(\mathbf{Y}_1)) \end{bmatrix}, \quad \mathbf{v}_1 = \begin{bmatrix} \text{vec}(\mathcal{R}(\mathbf{V}_1)) \\ \text{vec}(\mathcal{I}(\mathbf{V}_1)) \end{bmatrix}, \\ \tilde{\mathbf{s}} &= \begin{bmatrix} \mathcal{R}(\mathbf{s}) \\ \mathcal{I}(\mathbf{s}) \end{bmatrix}, \quad \text{and} \end{aligned} \quad (5)$$

$$\mathbf{H}_{e,1} = \begin{bmatrix} \text{vec}(\mathcal{R}(\mathbf{H}_1 \mathbf{C}_1)) & \text{vec}(\mathcal{I}(\mathbf{H}_1 \mathbf{C}_1)) \\ \vdots & \vdots \\ \text{vec}(\mathcal{R}(\mathbf{H}_1 \mathbf{C}_K)) & \text{vec}(\mathcal{I}(\mathbf{H}_1 \mathbf{C}_K)) \\ \text{vec}(\mathcal{R}(\mathbf{H}_1 \mathbf{D}_1)) & \text{vec}(\mathcal{I}(\mathbf{H}_1 \mathbf{D}_1)) \\ \vdots & \vdots \\ \text{vec}(\mathcal{R}(\mathbf{H}_1 \mathbf{D}_K)) & \text{vec}(\mathcal{I}(\mathbf{H}_1 \mathbf{D}_K)) \end{bmatrix}^T. \quad (6)$$

Note that \mathbf{y}_1 and \mathbf{v}_1 are of the size $2N_r T \times 1$, whereas $\mathbf{H}_{e,1}$ has a size of $2N_r T \times 2K$. In a similar way, we get $\mathbf{y}_3 = \mathbf{H}_{e,3} \tilde{\mathbf{s}} + \mathbf{v}_3$. Using the properties of the dispersion matrices, $\mathbf{H}_{e,1}^T \mathbf{H}_{e,1}$ and $\mathbf{H}_{e,3}^T \mathbf{H}_{e,3}$ are expressed as in [6]-[7] as

$$\mathbf{H}_{e,1}^T \mathbf{H}_{e,1} = \|\mathbf{H}_1\|_F^2 \mathbf{I}_{2K}, \quad \mathbf{H}_{e,3}^T \mathbf{H}_{e,3} = \|\mathbf{H}_3\|_F^2 \mathbf{I}_{2K}. \quad (7)$$

Let \mathbf{v}_1 be expressed as $\mathbf{v}_1 = [\mathcal{R}(\mathbf{v}_{1,1})^T, \dots, \mathcal{R}(\mathbf{v}_{1,T})^T, \mathcal{I}(\mathbf{v}_{1,1})^T, \dots, \mathcal{I}(\mathbf{v}_{1,T})^T]^T$, where $\mathbf{v}_{1,t}$, $t = 1, \dots, T$ is the t th column of \mathbf{V}_1 . Consider that the spatial correlation matrix of noise at the relay is $\bar{\mathbf{R}}_{\mathbf{v},1} \in \mathcal{C}^{N_r \times N_r}$. Then, we express $\mathbf{v}_{1,t}$ as $\mathbf{v}_{1,t} = \bar{\mathbf{R}}_{\mathbf{v},1}^{\frac{1}{2}} \tilde{\mathbf{v}}_{1,t}$ where the elements of $\tilde{\mathbf{v}}_{1,t}$ are considered to be independent and identically distributed (i.i.d.) zero-mean circularly

⁶This is a standard system model assumption used widely in the literature of cooperative communications. On the other hand, an exact performance analysis in the presence of both small-scale and shadow fading is not theoretically tractable for a MIMO AF relay system considered in this manuscript. This is due to the fact that we need to deal with the product of the functions of two random processes. The related complexity is also evident from [25] which limits the analysis to a single-antenna decode-and-forward relay system for obtaining the upper bound of the system symbol error rate.

symmetric complex Gaussian (ZMCSCG) random variables with unit variance. From (1a)-(1b), we get

$$\begin{aligned}\mathcal{R}(\bar{\mathbf{R}}_{\mathbf{v},1}^{\frac{1}{2}}\tilde{\mathbf{v}}_{1,t}) &= \left[\mathcal{R}(\bar{\mathbf{R}}_{\mathbf{v},1}^{\frac{1}{2}}), -\mathcal{I}(\bar{\mathbf{R}}_{\mathbf{v},1}^{\frac{1}{2}}) \right] \begin{bmatrix} \mathcal{R}(\tilde{\mathbf{v}}_{1,t}) \\ \mathcal{I}(\tilde{\mathbf{v}}_{1,t}) \end{bmatrix} \\ \mathcal{I}(\bar{\mathbf{R}}_{\mathbf{v},1}^{\frac{1}{2}}\tilde{\mathbf{v}}_{1,t}) &= \left[\mathcal{I}(\bar{\mathbf{R}}_{\mathbf{v},1}^{\frac{1}{2}}), \mathcal{R}(\bar{\mathbf{R}}_{\mathbf{v},1}^{\frac{1}{2}}) \right] \begin{bmatrix} \mathcal{R}(\tilde{\mathbf{v}}_{1,t}) \\ \mathcal{I}(\tilde{\mathbf{v}}_{1,t}) \end{bmatrix}.\end{aligned}$$

Thus, \mathbf{v}_1 is expressed as

$$\mathbf{v}_1 = \begin{bmatrix} \mathbf{I}_T \otimes \mathcal{R}(\bar{\mathbf{R}}_{\mathbf{v},1}^{\frac{1}{2}}) & -\mathbf{I}_T \otimes \mathcal{I}(\bar{\mathbf{R}}_{\mathbf{v},1}^{\frac{1}{2}}) \\ \mathbf{I}_T \otimes \mathcal{I}(\bar{\mathbf{R}}_{\mathbf{v},1}^{\frac{1}{2}}) & \mathbf{I}_T \otimes \mathcal{R}(\bar{\mathbf{R}}_{\mathbf{v},1}^{\frac{1}{2}}) \end{bmatrix} \begin{bmatrix} \mathcal{R}(\tilde{\mathbf{v}}_{1,1}) \\ \vdots \\ \mathcal{R}(\tilde{\mathbf{v}}_{1,T}) \\ \mathcal{I}(\tilde{\mathbf{v}}_{1,1}) \\ \vdots \\ \mathcal{I}(\tilde{\mathbf{v}}_{1,T}) \end{bmatrix}.$$

Since $\mathbb{E}\{\mathcal{R}(\tilde{\mathbf{v}}_{1,\bar{t}})\mathcal{R}(\tilde{\mathbf{v}}_{1,t})^T\} = \mathbf{0}$ and $\mathbb{E}\{\mathcal{I}(\tilde{\mathbf{v}}_{1,\bar{t}})\mathcal{I}(\tilde{\mathbf{v}}_{1,t})^T\} = \mathbf{0}$ for $t \neq \bar{t}$, and $\mathbb{E}\{\mathcal{R}(\tilde{\mathbf{v}}_{1,t})\mathcal{R}(\tilde{\mathbf{v}}_{1,t})^T\} = \mathbb{E}\{\mathcal{I}(\tilde{\mathbf{v}}_{1,t})\mathcal{I}(\tilde{\mathbf{v}}_{1,t})^T\} \triangleq \frac{1}{2}\mathbf{I}_{N_r}, \forall t$, we obtain

$$\mathbf{R}_{\mathbf{v},1} = \mathbb{E}\{\mathbf{v}_1\mathbf{v}_1^T\} = \frac{1}{2} \begin{bmatrix} \mathbf{I}_T \otimes \mathbf{R}_d & -\mathbf{I}_T \otimes \mathbf{R}_{nd} \\ \mathbf{I}_T \otimes \mathbf{R}_{nd} & \mathbf{I}_T \otimes \mathbf{R}_d \end{bmatrix}, \quad (8)$$

where

$$\begin{aligned}\mathbf{R}_d &= \mathcal{R}(\bar{\mathbf{R}}_{\mathbf{v},1}^{\frac{1}{2}})\mathcal{R}(\bar{\mathbf{R}}_{\mathbf{v},1}^{\frac{1}{2}})^T + \mathcal{I}(\bar{\mathbf{R}}_{\mathbf{v},1}^{\frac{1}{2}})\mathcal{I}(\bar{\mathbf{R}}_{\mathbf{v},1}^{\frac{1}{2}})^T \\ \mathbf{R}_{nd} &= \mathcal{I}(\bar{\mathbf{R}}_{\mathbf{v},1}^{\frac{1}{2}})\mathcal{R}(\bar{\mathbf{R}}_{\mathbf{v},1}^{\frac{1}{2}})^T - \mathcal{R}(\bar{\mathbf{R}}_{\mathbf{v},1}^{\frac{1}{2}})\mathcal{I}(\bar{\mathbf{R}}_{\mathbf{v},1}^{\frac{1}{2}})^T.\end{aligned} \quad (9)$$

The relay and destination nodes employ MMSE receivers. Consider the S-R MIMO channel. The estimated symbol is expressed as

$$\hat{\mathbf{s}}_r = \mathbf{Z}_1^T \mathbf{y}_1 = \mathbf{Z}_1^T (\mathbf{H}_{e,1}\tilde{\mathbf{s}} + \mathbf{v}_1), \quad (10)$$

where $\mathbf{Z}_1 \in \mathcal{R}^{2N_r T \times 2K}$ is a linear receiver at the relay. The MMSE receiver \mathbf{Z}_1 is given by

$$\mathbf{Z}_1 = (\mathbf{H}_{e,1}\mathbf{R}_{\tilde{\mathbf{s}}}\mathbf{H}_{e,1}^T + \mathbf{R}_{\mathbf{v},1})^{-1} \mathbf{H}_{e,1}\mathbf{R}_{\tilde{\mathbf{s}}} \quad (11)$$

where $\mathbf{R}_{\tilde{\mathbf{s}}} = \mathbb{E}\{\tilde{\mathbf{s}}\tilde{\mathbf{s}}^T\}$. Since $\mathbb{E}\{|s_k|^2\} = 1$ and $\mathbb{E}\{s_k s_k^*\} = 0, \forall k \neq \bar{k}$, we have $\mathbf{R}_{\tilde{\mathbf{s}}} = \frac{1}{2}\mathbf{I}_{2K}$. Thus, the MMSE estimate is given by

$$\hat{\mathbf{s}}_r = \mathbf{H}_{e,1}^T (\mathbf{H}_{e,1}\mathbf{H}_{e,1}^T + 2\mathbf{R}_{\mathbf{v},1})^{-1} (\mathbf{H}_{e,1}\tilde{\mathbf{s}} + \mathbf{v}_1). \quad (12)$$

After using the following matrix-identity [24]

$$\begin{aligned}(\mathbf{R}_{\mathbf{v},1} + \mathbf{H}_{e,1}\mathbf{H}_{e,1}^T)^{-1} \mathbf{H}_{e,1} &= \frac{1}{2}\mathbf{R}_{\mathbf{v},1}^{-1}\mathbf{H}_{e,1} \left[\mathbf{I} + \frac{1}{2}\mathbf{H}_{e,1}^T \right. \\ &\quad \left. \mathbf{R}_{\mathbf{v},1}^{-1}\mathbf{H}_{e,1} \right]^{-1}\end{aligned} \quad (13)$$

and defining $\mathbf{T} \triangleq \frac{1}{2}\mathbf{H}_{e,1}^T \mathbf{R}_{\mathbf{v},1}^{-1} \mathbf{H}_{e,1}$, the MMSE estimate (12) is given by

$$\hat{\mathbf{s}}_r = \mathbf{T}(\mathbf{I} + \mathbf{T})^{-1} \tilde{\mathbf{s}} + (\mathbf{I} + \mathbf{T})^{-1} \frac{1}{2}\mathbf{H}_{e,1}^T \mathbf{R}_{\mathbf{v},1}^{-1} \mathbf{v}_1. \quad (14)$$

We show that \mathbf{T} turns to a scaled identity matrix due to the properties of the OSTBC. This result is an extension of (7) which is a specific case with $\mathbf{R}_{\mathbf{v},1} = \mathbf{I}_{2N_r T}$ and proved in [7] using constellation space invariance property of OSTBC. Our result for general $\mathbf{R}_{\mathbf{v},1}$ is formulated in the following proposition which in other words establishes

the equivalency between the maximum-likelihood (ML) and MMSE receivers for an OSTBC-based MIMO system that is subject to correlated noise.

Proposition 1: The estimate $\hat{\mathbf{s}}_r$ of the relay is expressed in the following decoupled form as⁷

$$\hat{s}_{l,r} = \frac{\alpha_1}{1 + \alpha_1} \tilde{s}_l + \frac{1}{1 + \alpha_1} \tilde{v}_l, l = 1, \dots, 2K, \text{ where} \quad (15)$$

$$\alpha_1 = \text{tr}(\mathbf{H}_1 \mathbf{H}_1^H \bar{\mathbf{R}}_{\mathbf{v},1}^{-1}), \tilde{v}_l = \frac{1}{2} ([\mathbf{H}_{e,1}^T \mathbf{R}_{\mathbf{v},1}^{-1}]_{l,:}) \mathbf{v}_1. \quad (16)$$

Proof: Please refer to Appendix A. \square

The destination processes the signal received from the source with the MMSE receiver. Using the result of Proposition 1, the source signal estimated by the destination is given by

$$\hat{\mathbf{s}}_d = \frac{\alpha_3 \tilde{\mathbf{s}}}{1 + \alpha_3} + \frac{(1/2)\mathbf{H}_{e,3}^T \mathbf{R}_{\mathbf{v},2}^{-1} \mathbf{v}_3}{1 + \alpha_3}, \quad \alpha_3 = \text{tr}(\mathbf{H}_3 \mathbf{H}_3^H \bar{\mathbf{R}}_{\mathbf{v},2}^{-1}) \quad (17)$$

where $\mathbf{v}_3 \in \mathcal{R}^{2N_d T \times 1}$ is formed from \mathbf{V}_3 and defined as \mathbf{v}_1 in (5), and $\bar{\mathbf{R}}_{\mathbf{v},2} \in \mathcal{C}^{N_d \times N_d}$ is the correlation matrix of the destination noise. Moreover, $\mathbf{R}_{\mathbf{v},2} \in \mathcal{R}^{2N_d T \times 2N_d T}$ is the function of $\bar{\mathbf{R}}_{\mathbf{v},2}$ as given by (8) for the case with $\mathbf{R}_{\mathbf{v},1}$. The SNR of the S-D link is then given by

$$\gamma_3 = \alpha_3 = \text{tr}(\mathbf{H}_3 \mathbf{H}_3^H \bar{\mathbf{R}}_{\mathbf{v},2}^{-1}). \quad (18)$$

In the SR protocol, transmission via the relay takes place only when the S-D link fails to support the target rate, whereas in the FR protocol the relay is always used during the second phase of the transmission. The relay normalizes the estimated signal $\hat{s}_{l,r} \triangleq \hat{s}_{l,r} + j\hat{s}_{l+K,r}, l = 1, \dots, K$, encodes the normalized signal with the OSTBC and forwards the resulting signal to the destination. The power of the l th complex symbol received at the relay is given by

$$\begin{aligned}\mathbb{E}\{|\hat{s}_{l,r}|^2\} &= \frac{(\alpha_1^2 \mathbb{E}\{|\tilde{s}_l + j\tilde{s}_{l+K}|^2\} + \mathbb{E}\{|\tilde{v}_l + j\tilde{v}_{l+K}|^2\})}{(1 + \alpha_1)^2} \\ &= \frac{\alpha_1}{(1 + \alpha_1)},\end{aligned} \quad (19)$$

where we use the facts that $\mathbb{E}\{|\tilde{s}_l + j\tilde{s}_{l+K}|^2\} = 1$ and $\mathbb{E}\{|\tilde{v}_l|^2\} = \mathbb{E}\{|\tilde{v}_{l+K}|^2\} = \alpha_1$. The normalized l th complex symbol $\bar{y}_{l,r}$ at the relay is expressed as

$$\bar{y}_{l,r} = \sqrt{\frac{\alpha_1}{(1 + \alpha_1)}} \left((\tilde{s}_l + j\tilde{s}_{l+K}) + \frac{1}{\alpha_1} (\tilde{v}_l + j\tilde{v}_{l+K}) \right). \quad (20)$$

Let $\bar{\mathbf{y}}_r = [\bar{y}_{1,r}, \dots, \bar{y}_{K,r}]^T \in \mathcal{C}^{K \times 1}$. The relay employs OSTBC which is a function of $\bar{\mathbf{y}}_r$ as in (3) and transmits the resulting $N_r \times T$ signal to the destination. The $N_d \times T$ matrix of received signal samples at the destination is given by

$$\mathbf{Y}_2 = \sqrt{\frac{P_r \mu_2}{N_r}} \tilde{\mathbf{H}}_2 \mathbf{S}(\bar{\mathbf{y}}_r) + \mathbf{V}_2 = \mathbf{H}_2 \mathbf{S}(\bar{\mathbf{y}}_r) + \mathbf{V}_2 \quad (21)$$

where $\tilde{\mathbf{H}}_2$ is the normalized $N_d \times T$ R-D MIMO channel, μ_2 is the corresponding path gain, \mathbf{V}_2 is $N_d \times T$ matrix of

⁷Notice that the proposed analysis with the MMSE receiver is general since the derivations of this proposition can be straightforwardly extended to the case where interferers employ OSTBCs and their channels are known [26].

noise signals at the destination and $\mathbf{S}(\bar{\mathbf{y}}_r)$ is the $N_T \times T$ OSTBC formed from complex symbols $\bar{\mathbf{y}}_r$. The path gain μ_2 is given by $\mu_2 = d_2^{-\zeta}$, where d_2 is the R-D distance. The destination also employs MMSE receiver to decode the source signal from \mathbf{Y}_2 . Using Proposition 1, the estimated source signal at the destination is derived in the following proposition. This proposition in fact establishes equivalency between the ML and MMSE receivers for an OSTBC-MIMO relay system where noise at both relay and destination nodes are spatially correlated.

Proposition 2: The estimated source signal from \mathbf{Y}_2 is given by

$$\hat{s}_{l,d} = \frac{\tilde{\alpha} \tilde{s}_l}{\tilde{\alpha} + 1} + \frac{(1/2) \left([\bar{\mathbf{H}}_{e,2}^T \bar{\mathbf{R}}_{\tilde{\mathbf{v}}}^{-1}]_{l,:} \right) \tilde{\mathbf{v}}}{\tilde{\alpha} + 1}, l = 1, \dots, 2K, (22)$$

where $\tilde{\alpha} = \frac{\alpha_1 \alpha_2}{\alpha_1 + \alpha_2 + 1}$ and

$$\alpha_2 = \text{tr}(\mathbf{H}_2 \mathbf{H}_2^H \bar{\mathbf{R}}_{\mathbf{v},2}^{-1}), \bar{\mathbf{H}}_{e,2} = \sqrt{\frac{\alpha_1}{(1 + \alpha_1)}} \mathbf{H}_{e,2},$$

$$\tilde{\mathbf{v}} = \frac{\bar{\mathbf{H}}_{e,2} (1/2) \mathbf{H}_{e,1}^T \bar{\mathbf{R}}_{\mathbf{v},1}^{-1} \mathbf{v}_1}{\alpha_1} + \mathbf{v}_2, \bar{\mathbf{R}}_{\tilde{\mathbf{v}}} = \text{E} \{ \tilde{\mathbf{v}} \tilde{\mathbf{v}}^H \}, (23)$$

$\mathbf{v}_2 \in \mathcal{R}^{2N_d T \times 1}$ and $\mathbf{H}_{e,2} \in \mathcal{R}^{2N_d T \times 2K}$ are given as in (4)-(6).

Proof: Please refer to Appendix B. \square

From Proposition 2, the SNR of the S-R-D link is given by

$$\gamma_{1-2} = \frac{\text{tr}(\mathbf{H}_1 \mathbf{H}_1^H \bar{\mathbf{R}}_{\mathbf{v},1}^{-1}) \text{tr}(\mathbf{H}_2 \mathbf{H}_2^H \bar{\mathbf{R}}_{\mathbf{v},2}^{-1})}{\text{tr}(\mathbf{H}_1 \mathbf{H}_1^H \bar{\mathbf{R}}_{\mathbf{v},1}^{-1}) + \text{tr}(\mathbf{H}_2 \mathbf{H}_2^H \bar{\mathbf{R}}_{\mathbf{v},2}^{-1}) + 1}. (24)$$

It is clear from (22) that the estimated source symbols at the destination do not interfere with each other. As such, application of OSTBCs at the source and relay, and the linear MMSE receivers at the relay and destination makes symbol by symbol decoding possible. Therefore, the MMSE receivers are optimal.

IV. PERFORMANCE ANALYSIS

In this section, exact and asymptotic expressions of the outage probability are derived for the SR protocol, whereas the asymptotic expression is derived for the FR protocol⁸. Based on the asymptotic expressions, diversity gains are obtained for both protocols.

Using double-sided Kronecker's correlation model [27], the MIMO channels (S-R, R-D and S-D) are given by

$$\mathbf{H}_m = \sqrt{\eta_m} \mathbf{R}_{r,m}^{\frac{1}{2}} \mathbf{H}_{w,m} \mathbf{R}_{t,m}^{\frac{1}{2}}, m = 1, 2, 3, \eta_1 = \frac{P_s \mu_1}{N_s},$$

$$\eta_2 = \frac{P_r \mu_2}{N_r}, \eta_3 = \frac{P_s \mu_3}{N_s} (25)$$

where $\mathbf{R}_{r,m}$ and $\mathbf{R}_{t,m}$ are respectively, the receive-side and transmit-side correlation matrices for the i th MIMO channel⁹. The entries of $\mathbf{H}_{w,m}$ are assumed to be i.i.d. ZMCSCG random variables. Substituting \mathbf{H}_m from (25) into α_m yields $\alpha_m =$

⁸The derivation of the exact expression in the FR protocol turns to be mathematically intractable, and, as in the SR protocol, it is very much likely that such exact expression does not provide insights into diversity and CGs.

⁹The proposed performance analysis also holds true when mutual coupling matrices [22] are lumped to spatial channel correlation matrices.

$\eta_m \text{tr} \left(\mathbf{H}_{w,m}^H \mathbf{R}_{r,m}^{\frac{1}{2}} \bar{\mathbf{R}}_{\mathbf{v}_m}^{-1} \mathbf{R}_{r,m}^{\frac{1}{2}} \mathbf{H}_{w,m} \mathbf{R}_{t,m} \right)$, where $\bar{m} = m$ for $m = 1, 2$ and $\bar{m} = 2$ for $m = 3$. Using the facts that $\text{tr}(\mathbf{X}^H \mathbf{A} \mathbf{X} \mathbf{B}) = \text{vec}(\mathbf{X})^H \text{vec}(\mathbf{A} \mathbf{X} \mathbf{B}) = \text{vec}(\mathbf{X})^H (\mathbf{B}^T \otimes \mathbf{A}) \text{vec}(\mathbf{X})$ [24], we get

$$\alpha_m = \eta_m \text{vec}(\mathbf{H}_{w,m})^H \left[\mathbf{R}_{t,m}^T \otimes \left(\mathbf{R}_{r,m}^{\frac{1}{2}} \bar{\mathbf{R}}_{\mathbf{v}_m}^{-1} \mathbf{R}_{r,m}^{\frac{1}{2}} \right) \right] \text{vec}(\mathbf{H}_{w,m}). (26)$$

Define $\tilde{\Phi}_m \triangleq \mathbf{R}_{t,m}^T \otimes \left(\mathbf{R}_{r,m}^{\frac{1}{2}} \bar{\mathbf{R}}_{\mathbf{v}_m}^{-1} \mathbf{R}_{r,m}^{\frac{1}{2}} \right)$ and let $\tilde{\Phi}_m = \mathbf{U}_m \tilde{\Lambda}_m \mathbf{U}_m^H$ be the eigen decomposition of $\tilde{\Phi}_m$, where \mathbf{U}_m are the unitary matrices and $\tilde{\Lambda}_m$ are the diagonal matrices with the eigenvalues. α_m is expressed as

$$\alpha_m = (\text{vec}(\mathbf{H}_{w,m})^H \mathbf{U}_m) (\eta_m \tilde{\Lambda}_m) (\mathbf{U}_m^H \text{vec}(\mathbf{H}_{w,m}))$$

$$\triangleq \mathbf{h}_m^H \mathbf{\Lambda}_m \mathbf{h}_m (27)$$

where $\mathbf{\Lambda}_m = \eta_m \tilde{\Lambda}_m$ and $\mathbf{h}_m = \mathbf{U}_m^H \text{vec}(\mathbf{H}_{w,m})$. Since \mathbf{U}_m are unitary matrices, and the elements of $\text{vec}(\mathbf{H}_{w,m})$ are i.i.d. ZMCSCG random variables, the entries of \mathbf{h}_m remain i.i.d. ZMCSCG random. Let $\mathbf{\Lambda}_m = \text{diag} \left(\lambda_1^{(m)}, \dots, \lambda_{L_m}^{(m)}, 0, \dots, 0 \right)$, where $L_m = \text{rank}(\tilde{\Phi}_m)$. Then, α_m is written as $\alpha_m = \sum_{i=1}^{L_m} \lambda_i^{(m)} |h_i^m|^2$, where h_i^m is the i th element of \mathbf{h}_m . Since $h_i^m, \forall i$, are i.i.d. ZMCSCG with the unit variance, $|h_i^m|^2$ are exponentially distributed with the unit rate parameter. Consequently, $\alpha_m, \forall m$ are the weighted sum of the exponentially distributed random variables. Assuming that $\left\{ \lambda_i^{(m)} \right\}_{i=1}^{L_m}$ are distinct for a given m ¹⁰, the probability density function (PDF) of α_m is given by [28]

$$f_{\alpha_m}(z) = \sum_{i=1}^{L_m} a_i^{(m)} e^{-\frac{z}{\lambda_i^{(m)}}},$$

$$\text{with } a_i^{(m)} = \frac{(\lambda_i^{(m)})^{L_m-2}}{\prod_{j=1, j \neq i}^{L_m} \lambda_j^{(m)} - \lambda_j^{(m)}}. (28)$$

A. Outage Probability of Selection Relaying

Note that the transmission through the relay is employed only if the direct link is in outage, i.e., when $\ln_2(1 + \gamma_3) \leq r_t$. Therefore, the destination will be in outage if the relay is selected (i.e., direct link is in outage) and corresponding transmission is in outage. The outage probability at the destination is¹¹

$$P_o = \Pr \left\{ \frac{1}{2} \ln_2(1 + \gamma_{1-2}) \leq r_t, \ln_2(1 + \gamma_3) \leq r_t \right\}$$

$$= \Pr \{ \gamma_{1-2} \leq 2^{2r_t} - 1 \} \Pr \{ \gamma_3 \leq 2^{r_t} - 1 \}. (29)$$

Let us define $P_{o,1} = \Pr \left\{ \gamma_{1-2} \triangleq \frac{\alpha_1 \alpha_2}{1 + \alpha_1 + \alpha_2} \leq \tilde{r}_1 \right\}$ with $\tilde{r}_1 \triangleq 2^{2r_t} - 1$ and $P_{o,3} = \Pr \{ \gamma_3 \leq \tilde{r}_2 \}$ with $\tilde{r}_2 \triangleq 2^{r_t} - 1$. Using

¹⁰The assumption is made so that the difference between the SR and FR protocols can be analytically established in a comprehensive way. Nonetheless, due to the structure of eigenvalues of noise [17]-[22] and channel correlation matrices [29] in practice, the probability of having non-zero eigenvalues of multiplicity greater than one is minimum for $\tilde{\Phi}_m$ [24].

¹¹For notational clarity of the derivations, we consider full-rate OSTBC without loss of generality (w.l.o.g). Thus, the rate of the OSTBC does not appear in the expressions of performance analysis.

the PDF of α_3 , $P_{o,3}$ is expressed as

$$P_{o,3} = 1 - \sum_{l=1}^{L_3} a_l^{(3)} \lambda_l^{(3)} e^{-\frac{\tilde{r}_2}{\lambda_l^{(3)}}} \triangleq 1 - \tilde{P}_{o,3} \quad (30)$$

where we use the fact that $\sum_{l=1}^{L_3} a_l^{(3)} \lambda_l^{(3)} = 1$. We express $P_{o,1}$ as

$$\begin{aligned} P_{o,1} &= \int_0^\infty \Pr\{\alpha_1(x - \tilde{r}_1) \leq \tilde{r}_1(x+1)\} f_{\alpha_2}(x) dx \\ &= \int_0^{\tilde{r}_1} f_{\alpha_2}(x) dx + \int_{\tilde{r}_1}^\infty \Pr\left\{\alpha_1 \leq \frac{\tilde{r}_1(x+1)}{x - \tilde{r}_1}\right\} f_{\alpha_2}(x) dx \end{aligned}$$

where the last step is due to $\Pr\{\alpha_1(x - \tilde{r}_1) \leq x(\tilde{r}_1 + 1)\} = 1$ for $0 \leq x < \tilde{r}_1$. With the help of (28) and the relation $\sum_{i=1}^{L_1} a_i^{(1)} \lambda_i^{(1)} = 1$, we obtain

$$\Pr\left\{\alpha_1 \leq \frac{\tilde{r}_1(x+1)}{x - \tilde{r}_1}\right\} = 1 - \sum_{i=1}^{L_1} a_i^{(1)} \lambda_i^{(1)} e^{-\frac{\tilde{r}_1(x+1)}{(x - \tilde{r}_1)\lambda_i^{(1)}}}. \quad (31)$$

Using (31) and (28), the integral $I_2 \triangleq \int_{\tilde{r}_1}^\infty \Pr\left\{\alpha_1 \leq \frac{\tilde{r}_1(x+1)}{x - \tilde{r}_1}\right\} f_{\alpha_2}(x) dx$ is expressed as

$$\begin{aligned} I_2 &= \int_{\tilde{r}_1}^\infty f_{\alpha_2}(x) dx - \sum_{i=1}^{L_1} a_i^{(1)} \lambda_i^{(1)} \\ &\quad \times \int_{\tilde{r}_1}^\infty e^{-\frac{\tilde{r}_1(x+1)}{(x - \tilde{r}_1)\lambda_i^{(1)}}} f_{\alpha_2}(x) dx. \end{aligned} \quad (32)$$

Noting that $\int_0^{\tilde{r}_1} f_{\alpha_2}(x) dx + \int_{\tilde{r}_1}^\infty f_{\alpha_2}(x) dx = 1$, making a variable substitution $x' = x - \tilde{r}_1$ and applying [eq. (3.324.1), [30]], $P_{o,1}$ is given by¹²

$$P_{o,1} = 1 - \sum_{i=1}^{L_1} \sum_{k=1}^{L_2} a_i^{(1)} \lambda_i^{(1)} a_k^{(2)} \lambda_k^{(2)} e^{-\frac{\tilde{r}_1}{\lambda_i^{(1)}}} e^{-\frac{\tilde{r}_1}{\lambda_k^{(2)}}} \tilde{\beta}_{i,k} K_1(\tilde{\beta}_{i,k}), \quad (33)$$

where $\tilde{\beta}_{i,k} = 2\sqrt{\frac{\tilde{r}_1(\tilde{r}_1+1)}{\lambda_i^{(1)}\lambda_k^{(2)}}}$ and $K_1(\cdot)$ is the modified first-order Bessel function of the second type. Therefore, the closed-form expression for the outage probability $P_o = P_{o,1}P_{o,3} = P_{o,1} - P_{o,1}\tilde{P}_{o,3}$ is obtained. However, the exact expression remains complicated, and thus, sufficient metrics and the corresponding insights may not be obtained¹³. As such, we derive a novel asymptotic expression for P_o . Our key contribution in this regard is to carefully identify the properties of functions of the coefficients $a_i^{(m)}$ and exploit those properties to derive the asymptotic expressions that have simplified form and do not further depend on $a_i^{(m)}$.

1) Asymptotic analysis of selection relaying: We propose an asymptotic analysis (i.e., high SNR analysis) of P_o . Define $\mathbf{\Phi}_m \triangleq \mathbf{U}_m \tilde{\Lambda}_m^s (\mathbf{U}_m^s)^H$, where $\tilde{\Lambda}_m^s = \text{diag}(\lambda_1^{(m)}, \dots, \lambda_{L_m}^{(m)})$ is the diagonal matrix of non-zero eigenvalues of $\mathbf{\Phi}_m$ and \mathbf{U}_m^s is the matrix of columns of \mathbf{U}_m corresponding to these non-zero eigenvalues. Then, the main result is expressed in the following proposition.

¹²Note that when $L_1 = 1$ and $L_2 = 1$, $P_{o,1}$ reduces to the OP expression derived in [31] for a two-hop single-antenna AF relay channel.

¹³It is also difficult to use exact expression in optimization problems, for example, when $\{\lambda_i^{(1)}, \lambda_k^{(2)}, \lambda_i^{(3)}\}$ are the functions of the source and relay precoders [32].

Proposition 3: The outage probability of the SR protocol at high SNR is approximated as

$$P_o \approx \frac{c_2 c_3}{\eta_2^{L_2} \eta_3^{L_3} \det(\mathbf{\Phi}_2) \det(\mathbf{\Phi}_3)} + \frac{c_1 c_3}{\eta_1^{L_1} \eta_3^{L_3} \det(\mathbf{\Phi}_1) \det(\mathbf{\Phi}_3)} \quad (34)$$

where $c_m = \frac{\tilde{r}^{L_m}}{L_m!}$, $\tilde{r} = \tilde{r}_1$ for $m = 1, 2$, and $\tilde{r} = \tilde{r}_2$ for $m = 3$. *Proof:* Please refer to Appendix C. \square

Let $\{\eta_m\}_{m=1}^3$ be expressed in terms of $\rho \triangleq \frac{P_s}{N_s}$ as $\eta_m = \delta_m \rho$, $\forall m$, where $\delta_1 = d_1^{-\zeta}$, $\delta_2 = \bar{\delta}_2 d_2^{-\zeta}$ (with $\frac{P_r}{N_r} = \bar{\delta}_2 \rho$, $\bar{\delta}_2 > 0$) and $\delta_3 = d_3^{-\zeta}$. Substituting these values into (34), we obtain

$$\begin{aligned} P_o &\approx \frac{c_2 c_3}{\delta_2^{L_2} \delta_3^{L_3} \det(\mathbf{\Phi}_2) \det(\mathbf{\Phi}_3)} \rho^{-(L_2+L_3)} \\ &\quad + \frac{c_1 c_3}{\delta_1^{L_1} \delta_3^{L_3} \det(\mathbf{\Phi}_1) \det(\mathbf{\Phi}_3)} \rho^{-(L_1+L_3)} \\ &\approx \frac{c_{\hat{m}} c_3}{\delta_{\hat{m}}^{L_{\hat{m}}} \delta_3^{L_3} \det(\mathbf{\Phi}_{\hat{m}}) \det(\mathbf{\Phi}_3)} \rho^{-(L_{\hat{m}}+L_3)} \end{aligned} \quad (35)$$

where $\hat{m} = \arg \min_{1,2} \{L_1, L_2\}$. Comparing (35) with the standard asymptotic result $P_o \approx (G_c \rho)^{-G_d}$ [33], where G_c and G_d are respectively the coding and diversity gains, we find that the diversity order of the SR protocol is $\min(L_2 + L_3, L_1 + L_3)$. When all MIMO channels and noise are spatially uncorrelated, $L_1 = N_s N_r$, $L_2 = N_r N_d$, and $L_3 = N_s N_d$, i.e., the diversity gain of the SR protocol becomes $N_s N_d + \min(N_s N_r, N_r N_d)$ which, in fact, is the maximum diversity gain of a coherent MIMO relay system [14].

B. Asymptotic Analysis of Fixed Relaying

The FR protocol always uses the MIMO relay. In the first transmission phase, the source transmits, whereas the relay and destination listen to the source. In the second transmission phase, the relay transmits and the destination combines signals received from the source and destination. The outage probability of the FR protocol is therefore given by

$$P_{o,\text{fr}} = \Pr\left\{\frac{1}{2} \ln_2(1 + \gamma_{1-2} + \gamma_3) \leq r_t\right\}. \quad (36)$$

We derive a new asymptotic expression for $P_{o,\text{fr}}$ and determine the diversity gain of the FR protocol. Using the approximation that $\gamma_{1-2} = \frac{\alpha_1 \alpha_2}{\alpha_1 + \alpha_2 + 1} \approx \min(\alpha_1, \alpha_2)$ for high SNR regions, $P_{o,\text{fr}}$ is approximated as

$$\begin{aligned} P_{o,\text{fr}} &\approx \int_0^{\tilde{r}_1} \Pr\{\min(\alpha_1, \alpha_2) \leq \tilde{r}_1 - y\} f_{\alpha_3}(y) dy \\ &= \int_0^{\tilde{r}_1} [1 - \Pr\{\min(\alpha_1, \alpha_2) \geq \tilde{r}_1 - y\}] f_{\alpha_3}(y) dy, \quad (37) \\ &= \int_0^{\tilde{r}_1} [1 - \Pr\{\alpha_1 \geq \tilde{r}_1 - y\} \Pr\{\alpha_2 \geq \tilde{r}_1 - y\}] f_{\alpha_3}(y) dy \\ &= \int_0^{\tilde{r}_1} \left\{ \Pr\{\alpha_1 \leq \tilde{r}_1 - y\} + \Pr\{\alpha_2 \leq \tilde{r}_1 - y\} \right. \\ &\quad \left. - \Pr\{\alpha_1 \leq \tilde{r}_1 - y\} \Pr\{\alpha_2 \leq \tilde{r}_1 - y\} \right\} f_{\alpha_3}(y) dy. \end{aligned}$$

Since $\Pr\{\alpha_1 \leq \tilde{r}_1 - y\} = 1 - \sum_{i=1}^{L_1} a_i^{(1)} \lambda_i^{(1)} e^{-\frac{\tilde{r}_1 - y}{\lambda_i^{(1)}}}$ and $\Pr\{\alpha_2 \leq \tilde{r}_1 - y\} = 1 - \sum_{k=1}^{L_2} a_k^{(2)} \lambda_k^{(2)} e^{-\frac{\tilde{r}_1 - y}{\lambda_k^{(2)}}$, $P_{o,\text{fr}}$ in (37)

is expressed as

$$P_{o,fr} \approx \int_0^{\tilde{r}_1} \left[1 - \sum_{i=1}^{L_1} \sum_{k=1}^{L_2} a_i^{(1)} \lambda_i^{(1)} a_k^{(2)} \lambda_k^{(2)} e^{-\tilde{r}_1 \left(\frac{1}{\lambda_i^{(1)}} + \frac{1}{\lambda_k^{(2)}} \right)} \right] e^{y \left(\frac{1}{\lambda_i^{(1)}} + \frac{1}{\lambda_k^{(2)}} \right)} f_{\alpha_3}(y) dy. \quad (38)$$

Substituting $f_{\alpha_3}(y)$ into (38), $P_{o,fr}$ is re-expressed as

$$P_{o,fr} \approx 1 - \bar{P}_{o,3} - \sum_{i=1}^{L_1} \sum_{k=1}^{L_2} \sum_{l=1}^{L_3} \frac{a_i^{(1)} \lambda_i^{(1)} a_k^{(2)} \lambda_k^{(2)} a_l^{(3)}}{\tilde{\lambda}_{i,k,l}} \left[e^{-\tilde{r}_1 \frac{1}{\lambda_l^{(3)}}} - e^{-\tilde{r}_1 \left(\frac{1}{\lambda_i^{(1)}} + \frac{1}{\lambda_k^{(2)}} \right)} \right] \quad (39)$$

where $\tilde{\lambda}_{i,k,l} = \frac{1}{\lambda_i^{(1)}} + \frac{1}{\lambda_k^{(2)}} - \frac{1}{\lambda_l^{(3)}}$ and $\bar{P}_{o,3} = 1 - \sum_{l=1}^{L_3} a_l^{(3)} \lambda_l^{(3)} e^{-\frac{\tilde{r}_1}{\lambda_l^{(3)}}$. The final result of the asymptotic expansion for $P_{o,fr}$ is given in the following proposition¹⁴

Proposition 4: For high SNR, $P_{o,fr}$ is approximated as

$$P_{o,fr} \approx \frac{\tilde{r}_1^{L_1+L_3}}{(L_1+L_3)! \eta_1^{L_1} \eta_3^{L_3} \det(\Phi_1) \det(\Phi_3)} + \frac{\tilde{r}_1^{L_2+L_3}}{(L_2+L_3)! \eta_2^{L_2} \eta_3^{L_3} \det(\Phi_2) \det(\Phi_3)}. \quad (40)$$

Proof: Please refer to Appendix D. \square

As in the case of SR protocol, w.l.o.g., consider that $\eta_m = \delta_m \rho, \forall m$. Then, (40) is expressed as

$$P_{o,fr} \approx \frac{\tilde{r}_1^{L_{\hat{m}}+L_3}}{(L_{\hat{m}}+L_3)! \delta_{\hat{m}}^{L_{\hat{m}}} \delta_3^{L_3} \det(\Phi_{\hat{m}}) \det(\Phi_3)} \rho^{-(L_{\hat{m}}+L_3)}. \quad (41)$$

By comparing (41) with $P_{o,fr} \approx (G_c \rho)^{-G_d}$, we find that the diversity order of the FR protocol is also $\min(L_1+L_3, L_2+L_3)$. For uncorrelated channels and noise, the FR protocol achieves maximum diversity gain of $N_s N_d + \min(N_s N_r, N_r N_d)$ as in the SR protocol.

V. COMPARISON OF CODING GAINS

The CGs of the SR and FR protocols can be expressed, respectively, from (35) and (41) as

$$G_{c,1} = \left[\frac{\tilde{r}_1^{L_{\hat{m}}} \tilde{r}_2^{L_3}}{L_{\hat{m}}! L_3! \det(\Phi_{\hat{m}}) \det(\Phi_3)} \right]^{L_{\hat{m}}+L_3},$$

$$G_{c,2} = \left[\frac{\tilde{r}_1^{L_{\hat{m}}+L_3}}{(L_{\hat{m}}+L_3)! \det(\Phi_{\hat{m}}) \det(\Phi_3)} \right]^{L_{\hat{m}}+L_3}, \quad (42)$$

¹⁴The main contribution is to rigorously utilize the properties of functions of $a_i^{(m)}$ to derive a general simplified asymptotic expression that does not further depend on $a_i^{(m)}$. As it will be evident from Section V, the advantage of this contribution is that we are able to propose a comprehensive asymptotic analysis of the SR and FR protocols and provide important insights on their performance.

which means that the CG of the SR is better than that of the FR protocol if

$$\frac{\tilde{r}_1^{L_{\hat{m}}} \tilde{r}_2^{L_3}}{L_{\hat{m}}! L_3!} \leq \frac{\tilde{r}_1^{L_{\hat{m}}+L_3}}{(L_{\hat{m}}+L_3)!} \implies \frac{2^{r_t} - 1}{2^{2r_t} - 1} \leq \left(\frac{L_{\hat{m}}! L_3!}{(L_{\hat{m}}+L_3)!} \right)^{\frac{1}{L_3}}$$

$$\implies \frac{1}{2^{r_t} + 1} \leq \left(\frac{L_{\hat{m}}! L_3!}{(L_{\hat{m}}+L_3)!} \right)^{\frac{1}{L_3}}, \quad (43)$$

where the last step is due to $r_t > 0$. It is very difficult to simplify the term on the right-hand side of (43) for general values of $L_{\hat{m}}$ and L_3 . However, important insights can be obtained by analyzing (43) for some specific cases.

A. Case A: $L_{\hat{m}} = 1, L_3 \geq 1$

This is the case when one of the two-hop MIMO channels reduces to rank-one due to perfect spatial correlation or is a single-input single-output (SISO) channel. For this case, (43) simplifies to $\frac{1}{2^{r_t+1}} \leq \left(\frac{1}{L_3+1} \right)^{\frac{1}{L_3}}$. It can be readily shown that $\frac{1}{2} \leq \left(\frac{1}{L_3+1} \right)^{\frac{1}{L_3}} \leq 1$ for any $L_3 \geq 1$. This means that $G_{c,1} \leq G_{c,2}$ if $r_t > 0$. Consequently, the CG of the SR protocol is always better than that of the FR protocol in this case, and when all nodes are single-antenna nodes.

B. Case B: $L_{\hat{m}} = L_3 = L > 1$

In this case, the direct channel is as good as one of the two-hop links in terms of effective ranks. Using Stirling's approximation for a factorial of an integer (8.327.21 of [30]), $L!$ can be lower and upper bounded as

$$\sqrt{2\pi L} \left(\frac{L}{e_c} \right)^L \leq L! \leq e_c \sqrt{L} \left(\frac{L}{e_c} \right)^L \quad (44)$$

where $e_c \approx 2.718$ is Euler's number [30]. From (44), the following bounds are obtained

$$(L!L!)^{\frac{1}{L}} \geq \left(\sqrt{2\pi L} \left(\frac{L}{e_c} \right)^L \right)^{\frac{2}{L}},$$

$$((2L)!)^{\frac{1}{L}} \leq \left(e_c \sqrt{2L} \left(\frac{2L}{e_c} \right)^{2L} \right)^{\frac{1}{L}}, \quad (45)$$

which yield the following lower bound to $\left(\frac{L!L!}{(2L)!} \right)^{\frac{1}{L}}$

$$\left(\frac{L!L!}{(2L)!} \right)^{\frac{1}{L}} \geq \frac{1}{4} \left(\frac{\sqrt{2\pi}}{e_c} \right)^{\frac{2}{L}} L^{\frac{1}{2L}}. \quad (46)$$

Let $\bar{y} \triangleq s_c^{\frac{1}{L}} L^{\frac{1}{2L}}$ where $s_c = \frac{\sqrt{2\pi}}{e_c} \approx 1.634$. By plotting \bar{y} for $L \geq 1$, we easily observe that \bar{y} is a monotonically decreasing function of L . Alternatively, this can be verified from the first-order derivative of \bar{y} w.r.t. L . As such, the minimum value of \bar{y} is obtained when $L \rightarrow \infty$. It can be readily shown that $\bar{y} \rightarrow 1$ as $L \rightarrow \infty$. Therefore, (46) can be further lower bounded as $\left(\frac{L!L!}{(2L)!} \right)^{\frac{1}{L}} \geq \frac{1}{4}$. Consequently, the inequality in (43) can be further tightened as

$$\frac{1}{2^{r_t} + 1} \leq \frac{1}{4} \quad (47)$$

This means that, irrespective of the value of L , the CG of the SR protocol is better than that of the FR scheme as long as $r_t \geq \ln_2(3)$.

C. Case C: $L_3 = 1, L_{\tilde{m}} > 1$

This is the case when the S-D channel is in the worst-scenario when compared to the two-hop link in terms of rank. For this case, (43) simplifies to $\frac{1}{2^{r_t+1}} \leq \left(\frac{1}{L_{\tilde{m}}+1}\right)$. Note that $L_{\tilde{m}} \leq \min(N_s N_r, N_r N_d)$, i.e., the inequality is further tightened as $\frac{1}{2^{r_t+1}} \leq \left(\frac{1}{N_r \min(N_s, N_d) + 1}\right)$. For the desired full-rate OSTBCs (e.g., the Alamouti code), the number of antennas at transmit-side nodes turns to $N_r = N_s = 2$. Since $N_d = 1$ is implicitly included in Case A, we obtain $\frac{1}{2^{r_t+1}} \leq \frac{1}{5}$. This means that the CG of the SR protocol is better than that of the FR protocol if $r_t \geq 2$. With this analysis, we end this section with the following remarks.

Remark 1: When the effective rank of the S-D link is lower bounded by the minimum rank of the two-hop links, the SR protocol outperforms the FR protocol if the target information rate lies above zero or some small value (Cases A and B). However, when the S-D channel is in the worst-scenario (in terms of effective rank), depending on the value of $N_r \min(N_s, N_d)$, the SR protocol can be better than the FR only for larger values of r_t . Nevertheless, if Alamouti code is employed to avoid rate reduction, the CG of the SR protocol becomes better than the SR protocol with $r_t \geq 2$.

Remark 2: It is worthwhile to perform a large scale analysis of the proposed system having a large number of antennas at the source and relay nodes (i.e., $(N_s, N_r) \rightarrow \infty$). Since such analysis for a general case with spatially correlated channels and noise is much more involved and beyond the scope of this manuscript, we consider a case when channels and noise are spatially uncorrelated. Due to implementation and cost constraints at the destination node, N_d is assumed to be fixed. For the uncorrelated case, the end-to-end two-hop SNR is given by

$$\gamma_{1-2}^u = \frac{\eta_1 \eta_2 \text{tr}(\mathbf{H}_{w,1} \mathbf{H}_{w,1}^H) \text{tr}(\mathbf{H}_{w,2} \mathbf{H}_{w,2}^H)}{\eta_1 \text{tr}(\mathbf{H}_{w,1} \mathbf{H}_{w,1}^H) + \eta_2 \text{tr}(\mathbf{H}_{w,2} \mathbf{H}_{w,2}^H) + 1} \quad (48)$$

$$= \frac{a_1 \frac{\text{vec}(\mathbf{H}_{w,1})^H \text{vec}(\mathbf{H}_{w,1})}{N_s N_r} \frac{\text{vec}(\mathbf{H}_{w,2})^H \text{vec}(\mathbf{H}_{w,2})}{N_r N_d}}{a_2 \frac{\text{vec}(\mathbf{H}_{w,1})^H \text{vec}(\mathbf{H}_{w,1})}{N_s N_r} + a_3 \frac{\text{vec}(\mathbf{H}_{w,2})^H \text{vec}(\mathbf{H}_{w,2})}{N_r N_d} + 1}$$

where we use $\mathbf{R}_{r,m} = \mathbf{R}_{t,m} = \bar{\mathbf{R}}_{\tilde{v},\tilde{m}} = \mathbf{I}, \forall m, \tilde{m}$, $\text{tr}(\mathbf{H}_{w,m} \mathbf{H}_{w,m}^H) = \text{vec}(\mathbf{H}_{w,m})^H \text{vec}(\mathbf{H}_{w,m}), \forall m$, $a_1 = P_r P_s \mu_1 \mu_2 (N_r N_d)$, $a_2 = P_s \mu_1 N_r$, and $a_3 = P_r \mu_2 N_d$. The elements of $\text{vec}(\mathbf{H}_{w,m})$ are i.i.d. random variables with zero-mean and unit-variance. Applying the law of large numbers [34], we obtain

$$\frac{\text{vec}(\mathbf{H}_{w,1})^H \text{vec}(\mathbf{H}_{w,1})}{N_s N_r} \rightarrow 1, \text{ as } (N_s, N_r) \rightarrow \infty,$$

$$\frac{\text{vec}(\mathbf{H}_{w,2})^H \text{vec}(\mathbf{H}_{w,2})}{N_r N_d} \rightarrow 1, \text{ as } N_r \rightarrow \infty. \quad (49)$$

Substituting (49) into (48), the asymptotic value of γ_{1-2}^u is given by

$$\gamma_{1-2}^u \rightarrow \frac{P_r P_s \mu_1 \mu_2 (N_r N_d)}{P_s \mu_1 N_r + P_r \mu_2 N_d + 1} \text{ as } (N_s, N_r) \rightarrow \infty \quad (50)$$

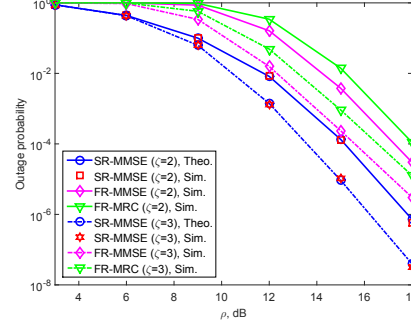


Fig. 2. Outage probability versus SNR for $r_t = 3$ b.p.c.u.

which after simple step reduces to

$$\gamma_{1-2}^u \rightarrow P_r \mu_2 N_d \text{ as } (N_s, N_r) \rightarrow \infty. \quad (51)$$

Similarly, using law of large numbers in $\gamma_3^u = \eta_3 \text{tr}(\mathbf{H}_{w,3} \mathbf{H}_{w,3}^H)$ as $N_s \rightarrow \infty$, γ_3^u is given by

$$\gamma_3^u \rightarrow P_s \mu_3 N_d \text{ as } N_s \rightarrow \infty. \quad (52)$$

As such, for $(N_s, N_r) \rightarrow \infty$ and fixed N_d , the SR protocol selects the relay only when $\ln_2(1 + P_s \mu_3 N_d) < r_t$, and outage occurs if both $\ln_2(1 + P_s \mu_3 N_d)$ and $\frac{1}{2} \ln_2(1 + P_r \mu_2 N_d)$ are smaller than r_t . However, in the FR protocol, the outage occurs if $\frac{1}{2} \ln_2(1 + (P_s \mu_3 + P_r \mu_2) N_d) < r_t$. It is interesting to note that as $(N_s, N_r) \rightarrow \infty$ and N_d is fixed, the outage depends only on N_d .

VI. NUMERICAL RESULTS

In this section, we provide Monte Carlo simulation results to assess the accuracy of the exact and asymptotic outage probability expressions. As a benchmark performance, we also show the performance of the FR protocol with the MRC receiver. The fast fading components of all MIMO channels, i.e., $\mathbf{H}_{w,m}, \forall m$ are taken from the entries of ZMCSG random variables with unit variances. Throughout all simulations, the S-D distance is normalized, i.e., $d_3 = 1$, whereas the S-R and R-D distances are respectively taken as $d_1 = 0.5d_3$ and $d_2 = 1 - d_1$. This means that the relay is located at the midpoint between the source and destination. The path loss exponent ζ takes the values of 2 and 3.

For all results, we take $P_s = P_r = P$, $n_s = n_r = n_d = 2$, and use Alamouti code. For comparing theoretical and simulation results, a common average SNR ρ is used, which is varied by changing P . In all simulations, we take $\bar{\mathbf{R}}_{v,1} = \bar{\mathbf{R}}_{v,2} = \begin{bmatrix} 1 & 0.5 \\ 0.5 & 1 \end{bmatrix}$ and exponential correlation models for channels, i.e., $\mathbf{R}_{r,m} = \mathbf{R}_{t,m} = \begin{bmatrix} 1 & \nu_m \\ \nu_m & 1 \end{bmatrix}$ with $\nu_m \geq 0$.

In Figs. 2 and 3, the outage probability versus SNR is displayed for the SR protocol, and the FR protocol that employs the MMSE and MRC receivers. We take $\nu_m = \nu = 0.4, \forall m$ in both figures, and $r_t = 3$ b.p.c.u and $r_t = 5$ b.p.c.u in Figs. 2 and 3, respectively. It can be observed from these figures that the SR method performs better than the FR protocol. In particular, at the outage probability of 10^{-2} , the SR protocol, respectively, provides gains of around 2.5 dB and 3.5 dB

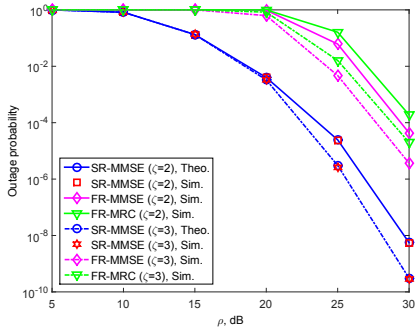


Fig. 3. Outage probability versus SNR for $r_t = 5$ b.p.c.u.

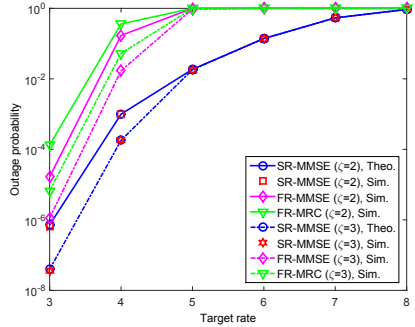


Fig. 4. Outage probability versus r_t for SNR=18 dB.

over the FR method with the MMSE and MRC receivers when $\zeta = 2$. These gains reduce to around 2 dB and 3 dB, respectively, when $\zeta = 3$ due to the fact that the attenuations of the S-R and R-D links decrease. As the value of r_t increases (e.g., from 3 to 5 b.p.c.u), the relative gain of the SR method over the FR-based methods improves further. For example, at the outage probability of 10^{-2} , the respective gains of the SR method over the FR-based MMSE and MRC methods are around 7.5 dB and 8.4 dB when $\zeta = 2$, and around 5.7 dB and 6.8 dB when $\zeta = 3$. Fig. 4 shows the outage probability versus r_t for different methods, where we fix ρ to 18 dB and take $\nu_m = \nu = 0.4, \forall m$. This figure also shows that the SR protocol outperforms the methods based on FR protocol. At the outage probability of 10^{-2} , the gains of the SR method over the FR method with the MMSE and MRC receivers are about 1.1 and 1.2 b.p.c.u, respectively, when $\zeta = 2$, and 0.9 and 1 b.p.c.u when $\zeta = 3$. This result also shows that when two-hop channel gains improve, the gain of the SR method over the FR-based schemes starts to decrease. In Fig. 5, the outage performance of different methods is depicted when the S-R and R-D channels observe much higher spatial correlation than the S-D channel. For this purpose, we take $\nu_m = 0.9, m = 1, 2$ and $\nu_3 = 0.1$. The target rate is set to $r_t = 3$ b.p.c.u. At the outage probability of 10^{-2} , the SR method provides around 2.7 dB and 3.2 dB improvements over the FR scheme with the MMSE and MRC receivers, respectively, when $\zeta = 2$. When $\zeta = 3$, these improvements reduce to around 1.8 dB and 2.5 dB, respectively. As in previous results, it is seen that the benefit of the SR method starts to shrink when the attenuations of the two-hop channels decrease.

The SR method is compared with the FR scheme employing MMSE and MRC receivers in Fig. 6 by considering that the

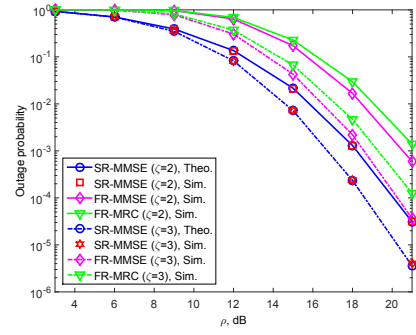


Fig. 5. Outage probability versus SNR for $r_t = 3$ b.p.c.u ($\nu_1 = \nu_2 = 0.9, \nu_3 = 0.1$).

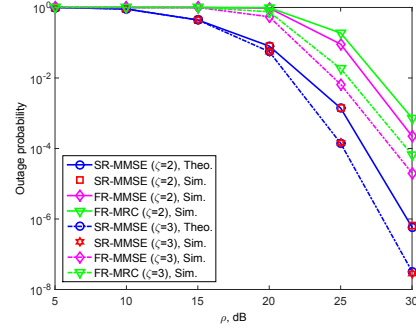


Fig. 6. Outage probability versus SNR for $r_t = 5$ b.p.c.u ($\nu_1 = \nu_2 = 0.1, \nu_3 = 0.9$).

S-D channel observes much higher spatial correlation than the S-R and R-D channels. As such, we take $\nu_3 = 0.9$ and $\nu_1 = \nu_2 = 0.1$. In this figure, the target rate is fixed to $r_t = 5$ b.p.c.u. For the outage probability of 10^{-2} , the respective gains of the SR method over the FR scheme with the MMSE and MRC receivers are about 4.25 dB and 5.1 dB when $\zeta = 2$, and 3.1 dB and 4.1 dB when $\zeta = 3$. As in Figs. 2-5, Fig. 6 shows that the gain of the SR method w.r.t. to the FR-based methods increase when path-loss exponent decreases from 3 to 2. In a nutshell, it can be observed from Figs. 5 and 6 that the SR method provides better performance than the FR methods in all of the considered examples. In Fig. 7, the asymptotic outage

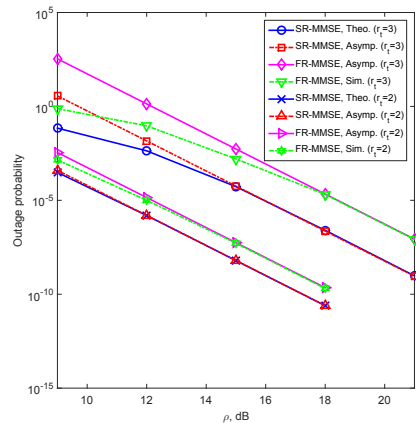


Fig. 7. Outage probability versus SNR for $r_t = 3, 2$ b.p.c.u.

probability expressions of the SR and FR protocols are shown for $r_t = 3$ b.p.c.u and $r_t = 2$ b.p.c.u. We take $\nu_m = 0.2, \forall m$ and $\zeta = 2$ in this figure. It can be observed from Fig. 7 that

the asymptotic outage probabilities of both protocols converge to corresponding actual outage probabilities as SNR increases. When r_t increases, the gap between the asymptotic and the actual outage probabilities increases in the low SNR region. However, it can be seen that the derived asymptotic outage probability of the SR protocol is much tighter than that of the FR protocol at low SNR region. Moreover, for a small value of r_t (e.g., $r_t = 0.8$), the FR protocol performs better than the SR protocol. The corresponding simulation results are not shown in this paper due to space constraints. However, all of these results are in accordance with the theoretical results of Section V.

We also investigate the relative performance difference between the SR and FR protocols for different relay positions. Although simulation results are not shown for conciseness, we find that the SR protocol significantly outperforms the FR-based methods for all positions of the relay, where the best performance of all methods is obtained when the relay is located at around the mid-point between the source and destination

VII. CONCLUSIONS

In this paper, selection relaying protocol is proposed for an OSTBC-based coherent AF MIMO relay system where the direct link between the source and the destination exists, and the channels and noise are spatially correlated. Asymptotic expressions of the outage probability are derived for the selection and fixed relaying protocols. It is shown that the performance of both protocols depends on the rank of a composite matrix which is a function of the channel and noise spatial correlation matrices. Moreover, both protocols achieve the same diversity gain. However, small values of target information rate can be sufficient for the selection relaying protocol to have better coding gain than the fixed relaying protocol. Simulation results show that the former protocol significantly outperforms the latter protocol with the MMSE and MRC receivers, especially for larger values of the target rate. These results may justify the complexity due to one-bit feedback requirement in the selection protocol. Moreover, the benefits of the selection relaying approach is much more pronounced when the attenuations of the two-hop channels increase.

APPENDIX A : PROOF OF PROPOSITION 1

Let $t(p, q)$ be the (p, q) th element of \mathbf{T} where $p, q = 1, \dots, 2K$. Then, $t(p, q)$ is expressed as

$$\begin{aligned} t(p, q) &= \frac{1}{2} \left[\text{vec} \left(\mathbf{H}_{1,R} \tilde{\mathbf{C}}_p \right)^T, \text{vec} \left(\mathbf{H}_{1,I} \tilde{\mathbf{C}}_p \right)^T \right] \mathbf{R}_{\mathbf{v},1}^{-1} \\ &\quad \times \left[\text{vec} \left(\mathbf{H}_{1,R} \tilde{\mathbf{C}}_q \right)^T, \text{vec} \left(\mathbf{H}_{1,I} \tilde{\mathbf{C}}_q \right)^T \right]^T \\ &= \frac{1}{2} \left[\text{vec}(\tilde{\mathbf{C}}_p)^T (\mathbf{I}_T \otimes \mathbf{H}_{1,R}^T), \text{vec}(\tilde{\mathbf{C}}_p)^T (\mathbf{I}_T \otimes \mathbf{H}_{1,I}^T) \right] \\ &\quad \times \mathbf{R}_{\mathbf{v},1}^{-1} \begin{bmatrix} (\mathbf{I}_T \otimes \mathbf{H}_{1,R}) \text{vec}(\tilde{\mathbf{C}}_q) \\ (\mathbf{I}_T \otimes \mathbf{H}_{1,I}) \text{vec}(\tilde{\mathbf{C}}_q) \end{bmatrix} \end{aligned} \quad (53)$$

where $\tilde{\mathbf{C}}_p = [\mathcal{R}(\mathbf{C}_p)^T, \mathcal{I}(\mathbf{C}_p)^T]^T$, $\mathbf{H}_{1,R} = [\mathcal{R}(\mathbf{H}_1), -\mathcal{I}(\mathbf{H}_1)]$, $\mathbf{H}_{1,I} = [\mathcal{I}(\mathbf{H}_1), \mathcal{R}(\mathbf{H}_1)]$, and we

have used (1a)-(1b) and (1d). For a positive definite matrix \mathbf{X} of complex values, we know that

$$\begin{bmatrix} \mathcal{R}(\mathbf{X}) & -\mathcal{I}(\mathbf{X}) \\ \mathcal{I}(\mathbf{X}) & \mathcal{R}(\mathbf{X}) \end{bmatrix}^{-1} = \begin{bmatrix} \mathcal{R}(\mathbf{X}^{-1}) & -\mathcal{I}(\mathbf{X}^{-1}) \\ \mathcal{I}(\mathbf{X}^{-1}) & \mathcal{R}(\mathbf{X}^{-1}) \end{bmatrix}. \quad (54)$$

Using (54), we express $\mathbf{R}_{\mathbf{v},1}^{-1}$ as

$$\mathbf{R}_{\mathbf{v},1}^{-1} = 2 \begin{bmatrix} \mathbf{I}_T \otimes \mathcal{R}(\tilde{\mathbf{R}}_{\mathbf{v},1}^{-1}) & -\mathbf{I}_T \otimes \mathcal{I}(\tilde{\mathbf{R}}_{\mathbf{v},1}^{-1}) \\ \mathbf{I}_T \otimes \mathcal{I}(\tilde{\mathbf{R}}_{\mathbf{v},1}^{-1}) & \mathbf{I}_T \otimes \mathcal{R}(\tilde{\mathbf{R}}_{\mathbf{v},1}^{-1}) \end{bmatrix}, \quad (55)$$

where we use the fact that $\tilde{\mathbf{R}}_{\mathbf{v},1} = \mathbf{R}_d + j\mathbf{R}_{nd}$. Substituting $\mathbf{R}_{\mathbf{v},1}^{-1}$ from (55) into (53), using (1e) and after some simplifications, we express $t(p, q)$ as

$$t(p, q) = \text{vec}(\tilde{\mathbf{C}}_p)^T [\mathbf{I}_T \otimes \tilde{\mathbf{H}}_1] \text{vec}(\tilde{\mathbf{C}}_q), \quad (56)$$

where

$$\tilde{\mathbf{H}}_1 = [\mathbf{H}_{1,R}^T, \mathbf{H}_{1,I}^T] \begin{bmatrix} \mathcal{R}(\tilde{\mathbf{R}}_{\mathbf{v},1}^{-1}) & -\mathcal{I}(\tilde{\mathbf{R}}_{\mathbf{v},1}^{-1}) \\ \mathcal{I}(\tilde{\mathbf{R}}_{\mathbf{v},1}^{-1}) & \mathcal{R}(\tilde{\mathbf{R}}_{\mathbf{v},1}^{-1}) \end{bmatrix} \begin{bmatrix} \mathbf{H}_{1,R} \\ \mathbf{H}_{1,I} \end{bmatrix}.$$

Applying (1d) and (1c) to (56), $t(p, q)$ is re-expressed as

$$t(p, q) = \text{tr} \left(\tilde{\mathbf{C}}_p \tilde{\mathbf{C}}_q^T \tilde{\mathbf{H}}_1 \right) = \begin{cases} \text{tr}(\mathbf{H}_1 \mathbf{H}_1^H \tilde{\mathbf{R}}_{\mathbf{v},1}^{-1}), & p = q \\ 0, & p \neq q \end{cases} \quad (57)$$

where the last equality is due to the properties of the dispersion matrices. The same result can be shown for $(p, q) = K + 1, \dots, 2K$, i.e., for the terms including $\mathbf{D}_p \mathbf{D}_q^T$ and $\mathbf{C}_p \mathbf{D}_q^T$. Therefore, \mathbf{T} reduces to the following scaled identity matrix

$$\mathbf{T} = \text{tr}(\mathbf{H}_1 \mathbf{H}_1^H \tilde{\mathbf{R}}_{\mathbf{v},1}^{-1}) \mathbf{I}_{2K}. \quad (58)$$

Substituting (58) into (14), $\hat{\mathbf{s}}_r$ is expressed as

$$\hat{\mathbf{s}}_r = \frac{\text{tr}(\mathbf{H}_1 \mathbf{H}_1^H \tilde{\mathbf{R}}_{\mathbf{v},1}^{-1})}{1 + \text{tr}(\mathbf{H}_1 \mathbf{H}_1^H \tilde{\mathbf{R}}_{\mathbf{v},1}^{-1})} \tilde{\mathbf{s}} + \frac{(1/2) \mathbf{H}_{e,1}^T \mathbf{R}_{\mathbf{v},1}^{-1} \mathbf{v}_1}{1 + \text{tr}(\mathbf{H}_1 \mathbf{H}_1^H \tilde{\mathbf{R}}_{\mathbf{v},1}^{-1})}, \quad (59)$$

which means that the l th element ($l = 1, \dots, 2K$) of $\hat{\mathbf{s}}_r$ is

$$\hat{s}_{l,r} = \frac{\alpha_1}{1 + \alpha_1} \tilde{s}_l + \frac{1}{1 + \alpha_1} ((1/2) [\mathbf{H}_{e,1}^T \mathbf{R}_{\mathbf{v},1}^{-1}]_{l,:}) \mathbf{v}_1, \quad (60)$$

where \tilde{s}_l is the l th element of $\tilde{\mathbf{s}} \triangleq [\tilde{s}_1, \dots, \tilde{s}_K, \tilde{s}_{K+1}, \dots, \tilde{s}_{2K}]^T$. This completes the proof of Proposition 1. \square

APPENDIX B : PROOF OF PROPOSITION 2

Using similar steps as (4)-(6) for the S-R MIMO channel, (21) is expressed in vector form as

$$\begin{aligned} \mathbf{y}_2 &= \mathbf{H}_{e,2} \tilde{\mathbf{y}}_r + \mathbf{v}_2, \quad \text{where} \\ \tilde{\mathbf{y}}_r &= \sqrt{\frac{\alpha_1}{(1 + \alpha_1)}} \tilde{\mathbf{s}} + \sqrt{\frac{1}{\alpha_1(1 + \alpha_1)}} \frac{1}{2} \mathbf{H}_{e,1}^T \mathbf{R}_{\mathbf{v},1}^{-1} \mathbf{v}_1, \end{aligned} \quad (61)$$

and $\mathbf{y}_2 \in \mathcal{R}^{2N_d T \times 1}$ is given as in (4)-(6). Using $\tilde{\mathbf{y}}_r$, \mathbf{y}_2 in (61) is expressed as

$$\begin{aligned} \mathbf{y}_2 &= \mathbf{H}_{e,2} \tilde{\mathbf{s}} \sqrt{\frac{\alpha_1}{(1 + \alpha_1)}} + \sqrt{\frac{1}{\alpha_1(1 + \alpha_1)}} \mathbf{H}_{e,2} \frac{1}{2} \mathbf{H}_{e,1}^T \\ &\quad \mathbf{R}_{\mathbf{v},1}^{-1} \mathbf{v}_1 + \mathbf{v}_2 = \tilde{\mathbf{H}}_{e,2} \tilde{\mathbf{s}} + \tilde{\mathbf{v}}. \end{aligned} \quad (62)$$

Note that $\mathbf{R}_{\tilde{\mathbf{v}}}$ is given by

$$\begin{aligned}\mathbf{R}_{\tilde{\mathbf{v}}} &= \frac{1}{4\alpha_1^2} \bar{\mathbf{H}}_{e,2} \mathbf{H}_{e,1}^T \mathbf{R}_{\mathbf{v},1}^{-1} \mathbf{H}_{e,1} \bar{\mathbf{H}}_{e,2}^T + \mathbf{R}_{\mathbf{v},2} \\ &= \frac{1}{2\alpha_1} \bar{\mathbf{H}}_{e,2} \bar{\mathbf{H}}_{e,2}^T + \mathbf{R}_{\mathbf{v},2}\end{aligned}\quad (63)$$

where $\mathbf{R}_{\mathbf{v},2} \in \mathcal{R}^{2N_d T \times 2N_d T}$ is a function of $\bar{\mathbf{R}}_{\mathbf{v},2}$ and given as in (8)-(9). Using the steps (10)-(14), the MMSE estimate of the source signal at the destination is given by

$$\hat{\mathbf{s}}_d = \tilde{\mathbf{T}} \left[\mathbf{I} + \tilde{\mathbf{T}} \right]^{-1} \tilde{\mathbf{s}} + \left[\mathbf{I} + \tilde{\mathbf{T}} \right]^{-1} \frac{1}{2} \bar{\mathbf{H}}_{e,2}^T \mathbf{R}_{\tilde{\mathbf{v}}}^{-1} \tilde{\mathbf{v}} \quad (64)$$

where $\tilde{\mathbf{T}} = \frac{1}{2} \bar{\mathbf{H}}_{e,2}^T \mathbf{R}_{\tilde{\mathbf{v}}}^{-1} \bar{\mathbf{H}}_{e,2}$. Using (63) and (13), $\tilde{\mathbf{T}}$ is expressed as

$$\begin{aligned}\tilde{\mathbf{T}} &= \frac{1}{2} \bar{\mathbf{H}}_{e,2}^T \left[\frac{1}{2\alpha_1} \bar{\mathbf{H}}_{e,2} \bar{\mathbf{H}}_{e,2}^T + \mathbf{R}_{\mathbf{v},2} \right]^{-1} \bar{\mathbf{H}}_{e,2} = \frac{\alpha_1}{1 + \alpha_1} \\ &\quad \frac{1}{2} \mathbf{H}_{e,2}^T \mathbf{R}_{\mathbf{v},2}^{-1} \mathbf{H}_{e,2} \left[\mathbf{I}_{2K} + \frac{1}{1 + \alpha_1} \frac{1}{2} \mathbf{H}_{e,2}^T \mathbf{R}_{\mathbf{v},2}^{-1} \mathbf{H}_{e,2} \right]^{-1}\end{aligned}\quad (65)$$

With the help of (53)-(57), $\frac{1}{2} \mathbf{H}_{e,2}^T \mathbf{R}_{\mathbf{v},2}^{-1} \mathbf{H}_{e,2}$ is expressed as

$$\frac{1}{2} \mathbf{H}_{e,2}^T \mathbf{R}_{\mathbf{v},2}^{-1} \mathbf{H}_{e,2} = \text{tr} \left(\mathbf{H}_2 \mathbf{H}_2^H \bar{\mathbf{R}}_{\mathbf{v},2}^{-1} \right) \mathbf{I}_{2K} \triangleq \alpha_2 \mathbf{I}_{2K}. \quad (66)$$

Therefore, we get $\tilde{\mathbf{T}} = \frac{\alpha_1 \alpha_2}{\alpha_1 + \alpha_2 + 1} \mathbf{I}_{2K} = \tilde{\alpha} \mathbf{I}_{2K}$. Consequently, the estimated signal at the destination is

$$\hat{\mathbf{s}}_d = \frac{\tilde{\alpha}}{\tilde{\alpha} + 1} \tilde{\mathbf{s}} + \frac{1}{\tilde{\alpha} + 1} (1/2) \bar{\mathbf{H}}_{e,2}^T \mathbf{R}_{\tilde{\mathbf{v}}}^{-1} \tilde{\mathbf{v}}, \quad (67)$$

which yields (22) with $\hat{\mathbf{s}}_d \triangleq [\hat{s}_{1,d}, \dots, \hat{s}_{2K,d}]^T$. This completes the proof of the Proposition 2. \square

APPENDIX C : PROOF OF PROPOSITION 3

For high SNR regions, $K_1(x)$ can be approximated by $\frac{1}{x}$. Consequently, $P_{o,1}$ is expressed as

$$\begin{aligned}P_{o,1} &\approx 1 - \sum_{i=1}^{L_1} a_i^{(1)} \lambda_i^{(1)} e^{-\frac{\tilde{r}_1}{\lambda_i^{(1)}}} \sum_{k=1}^{L_2} a_k^{(2)} \lambda_k^{(2)} e^{-\frac{\tilde{r}_1}{\lambda_k^{(2)}}} \\ &= 1 - \tilde{P}_{o,1} \tilde{P}_{o,2}\end{aligned}$$

where $\tilde{P}_{o,1}$ and $\tilde{P}_{o,2}$ are, respectively, the functions of $\lambda_i^{(1)}$ and $\lambda_k^{(2)}$. Noting that $e^{-x} = \sum_{n=0}^{\infty} \frac{(-1)^n x^n}{n!}$, $\tilde{P}_{o,m}$ is expressed as

$$\begin{aligned}\tilde{P}_{o,m} &= \sum_{i=1}^{L_m} a_i^{(m)} \lambda_i^{(m)} - \tilde{r} \sum_{i=1}^{L_m} a_i^{(m)} + \frac{1}{2} (\tilde{r})^2 \sum_{i=1}^{L_m} \frac{a_i^{(m)}}{\lambda_i^{(1)}} \\ &\quad - \frac{1}{6} (\tilde{r})^3 \sum_{i=1}^{L_m} \frac{a_i^{(m)}}{(\lambda_i^{(m)})^2} + \mathcal{O} \left(\frac{1}{\lambda_i^{(m)}} \right), m = 1, 2, 3, (68)\end{aligned}$$

where $\tilde{r} = \tilde{r}_1$ for $m = 1, 2$, $\tilde{r} = \tilde{r}_2$ for $m = 3$, and $\mathcal{O}(x)$ stands for higher-order terms of x . Resubstituting $a_i^{(m)}$ from (28) into (68), and after some simple steps of derivations, we find that the first two terms (denoted by $\tilde{l} = 0, 1$) of (68) reduce to $\sum_{i=1}^{L_m} a_i^{(m)} \lambda_i^{(m)} = 1$, $\sum_{i=1}^{L_m} a_i^{(m)} = 0$, whereas the terms corresponding to $\tilde{l} = 2$ and $\tilde{l} = 3$ yield

$$\sum_{i=1}^{L_m} \frac{a_i^{(m)}}{(\lambda_i^{(m)})^{\tilde{l}-1}} = \begin{cases} 0 & \text{for } \tilde{l} < L_m \\ \frac{(-1)^{\tilde{l}-1}}{\prod_{i=1}^{L_m} \lambda_i^{(m)}} & \text{for } \tilde{l} = L_m \end{cases} \cdot (69)$$

With the help of (69), $\tilde{P}_{o,m}$ is approximated at high-SNR region as

$$\tilde{P}_{o,m} \approx 1 - c_m \frac{1}{\prod_{i=1}^{L_m} \lambda_i^{(1)}} = 1 - c_m \frac{1}{\eta_m^{L_m} \det(\Phi_m)} \quad (70)$$

where $c_m = \frac{\tilde{r}^{L_m}}{L_m!}$. Therefore, the outage probability of the SR protocol at high SNR is approximated as

$$\begin{aligned}P_o &\approx \left(1 - \left(1 - c_1 \frac{1}{\eta_1^{L_1} \det(\Phi_1)} \right) \left(1 - c_2 \frac{1}{\eta_2^{L_2} \det(\Phi_2)} \right) \right) \\ &\quad \times c_3 \frac{1}{\eta_3^{L_3} \det(\Phi_3)} \\ &= \frac{c_2 c_3}{\eta_2^{L_2} \eta_3^{L_3} \det(\Phi_2) \det(\Phi_3)} + \frac{c_1 c_3}{\eta_1^{L_1} \eta_3^{L_3} \det(\Phi_1) \det(\Phi_3)} \\ &\quad - \prod_{m=1}^3 \frac{c_m}{\eta_m^{L_m} \det(\Phi_m)},\end{aligned}\quad (71)$$

from which (34) follows. \square

APPENDIX D : PROOF OF PROPOSITION 4

Noting that $e^{-x} = \sum_{n=0}^{\infty} \frac{(-1)^n x^n}{n!}$, we express $t \triangleq e^{-\tilde{r}_1 \frac{1}{\lambda_i^{(3)}}} - e^{-\tilde{r}_1 \left(\frac{1}{\lambda_i^{(1)}} + \frac{1}{\lambda_k^{(2)}} \right)}$ as

$$\begin{aligned}t &= \tilde{r}_1 \tilde{\lambda}_{i,k,l} - \frac{\tilde{r}_1^2}{2} \tilde{\lambda}_{i,k,l} \left(\frac{1}{\lambda_i^{(1)}} + \frac{1}{\lambda_k^{(2)}} + \frac{1}{\lambda_l^{(3)}} \right) \\ &\quad + \frac{\tilde{r}_1^3}{6} \tilde{\lambda}_{i,k,l} \left(\tilde{\lambda}_{i,k,l}^2 + 3 \left(\frac{1}{\lambda_i^{(1)}} + \frac{1}{\lambda_k^{(2)}} \right) \frac{1}{\lambda_l^{(3)}} \right) - \frac{\tilde{r}_1^4}{24} \tilde{\lambda}_{i,k,l} \\ &\quad \left[\frac{1}{\lambda_i^{(1)}} + \frac{1}{\lambda_k^{(2)}} + \frac{1}{\lambda_l^{(3)}} \right] \left[\left(\frac{1}{\lambda_i^{(1)}} + \frac{1}{\lambda_k^{(2)}} \right)^2 + \frac{1}{(\lambda_l^{(3)})^2} \right] \\ &\quad + \mathcal{O} \left(\frac{1}{\lambda_i^{(m)}} \right).\end{aligned}\quad (72)$$

Define $t_1 \triangleq \tilde{r}_1 \tilde{\lambda}_{i,k,l}$ and $t_2 \triangleq \frac{\tilde{r}_1^2}{2} \tilde{\lambda}_{i,k,l} \left(\frac{1}{\lambda_i^{(1)}} + \frac{1}{\lambda_k^{(2)}} + \frac{1}{\lambda_l^{(3)}} \right)$. Note that in the following steps, we often use the property

$$\sum_{i=1}^{L_m} a_i^{(m)} = 0, \sum_{i=1}^{L_m} a_i^{(m)} \lambda_i^{(m)} = 1, \forall m. \quad (73)$$

Applying (73), it can be shown that

$$\begin{aligned}&\sum_{i=1}^{L_1} \sum_{k=1}^{L_2} \sum_{l=1}^{L_3} \frac{a_i^{(1)} \lambda_i^{(1)} a_k^{(2)} \lambda_k^{(2)} a_l^{(3)}}{\tilde{\lambda}_{i,k,l}} t_1 = 0, \\ &\sum_{i=1}^{L_1} \sum_{k=1}^{L_2} \sum_{l=1}^{L_3} \frac{a_i^{(1)} \lambda_i^{(1)} a_k^{(2)} \lambda_k^{(2)} a_l^{(3)}}{\tilde{\lambda}_{i,k,l}} t_2 = \frac{\tilde{r}_1^2}{2} \sum_{i=1}^{L_1} \sum_{k=1}^{L_2} \sum_{l=1}^{L_3} a_i^{(1)} \\ &\quad \times \lambda_i^{(1)} a_k^{(2)} \lambda_k^{(2)} a_l^{(3)} \left(\frac{1}{\lambda_i^{(1)}} + \frac{1}{\lambda_k^{(2)}} + \frac{1}{\lambda_l^{(3)}} \right).\end{aligned}\quad (74)$$

Let $t_3 \triangleq \frac{\tilde{r}_1^3}{6} \tilde{\lambda}_{i,k,l} \left(\tilde{\lambda}_{i,k,l}^2 + 3 \left(\frac{1}{\lambda_i^{(1)}} + \frac{1}{\lambda_k^{(2)}} \right) \frac{1}{\lambda_l^{(3)}} \right)$. After some steps of derivations, we obtain

$$\begin{aligned} \sum_{i=1}^{L_1} \sum_{k=1}^{L_2} \sum_{l=1}^{L_3} \frac{a_i^{(1)} \lambda_i^{(1)} a_k^{(2)} \lambda_k^{(2)} a_l^{(3)}}{\tilde{\lambda}_{i,k,l}} t_3 &= \frac{\tilde{r}_1^3}{6} \sum_{i=1}^{L_1} \sum_{k=1}^{L_2} \sum_{l=1}^{L_3} a_i^{(1)} \\ &\times \lambda_i^{(1)} a_k^{(2)} \lambda_k^{(2)} a_l^{(3)} \left\{ \left(\frac{1}{\lambda_i^{(1)}} + \frac{1}{\lambda_k^{(2)}} \right)^2 + \right. \\ &\left. \left(\frac{1}{\lambda_i^{(1)}} + \frac{1}{\lambda_k^{(2)}} \right) \frac{1}{\lambda_l^{(3)}} + \frac{1}{(\lambda_l^{(3)})^2} \right\}. \end{aligned} \quad (75)$$

With the definition $t_4 \triangleq \frac{\tilde{r}_1^4}{24} \tilde{\lambda}_{i,k,l} \left[\frac{1}{\lambda_i^{(1)}} + \frac{1}{\lambda_k^{(2)}} + \frac{1}{\lambda_l^{(3)}} \right] \left[\left(\frac{1}{\lambda_i^{(1)}} + \frac{1}{\lambda_k^{(2)}} \right)^2 + \frac{1}{(\lambda_l^{(3)})^2} \right]$, we get

$$\begin{aligned} \sum_{i=1}^{L_1} \sum_{k=1}^{L_2} \sum_{l=1}^{L_3} \frac{a_i^{(1)} \lambda_i^{(1)} a_k^{(2)} \lambda_k^{(2)} a_l^{(3)}}{\tilde{\lambda}_{i,k,l}} t_4 &= \frac{\tilde{r}_1^4}{24} \sum_{i=1}^{L_1} \sum_{k=1}^{L_2} \sum_{l=1}^{L_3} a_i^{(1)} \\ &\times \lambda_i^{(1)} a_k^{(2)} \lambda_k^{(2)} a_l^{(3)} \left\{ \left(\frac{1}{\lambda_i^{(1)}} + \frac{1}{\lambda_k^{(2)}} \right)^3 + \frac{1}{(\lambda_l^{(3)})^3} \right. \\ &\left. \left(\frac{1}{\lambda_i^{(1)}} + \frac{1}{\lambda_k^{(2)}} \right) \frac{1}{(\lambda_l^{(3)})^2} + \left(\frac{1}{\lambda_i^{(1)}} + \frac{1}{\lambda_k^{(2)}} \right)^2 \frac{1}{\lambda_l^{(3)}} \right\}. \end{aligned} \quad (76)$$

On the other hand, using (73) and $e^{-x} = \sum_{n=0}^{\infty} \frac{(-1)^n x^n}{n!}$, $\bar{P}_{o,3}$ is expressed as

$$\bar{P}_{o,3} = - \sum_{l=1}^{L_3} a_l^{(3)} \lambda_l^{(3)} \sum_{n=2}^{\infty} \frac{(-1)^n \tilde{r}_1^n}{n! (\lambda_l^{(3)})^n}. \quad (77)$$

With the help of (72)-(76) and (77), $P_{o,fr}$ is generalized to

$$\begin{aligned} P_{o,fr} &\approx \sum_{n=2}^{\infty} \frac{\tilde{r}_1^n}{n!} \sum_{i=1}^{L_1} \sum_{k=1}^{L_2} \sum_{l=1}^{L_3} a_i^{(1)} \lambda_i^{(1)} a_k^{(2)} \lambda_k^{(2)} a_l^{(3)} \\ &\left\{ \left(\frac{1}{\lambda_i^{(1)}} + \frac{1}{\lambda_k^{(2)}} \right)^{n-2} \right. \\ &\frac{1}{(\lambda_l^{(3)})} + \left(\frac{1}{\lambda_i^{(1)}} + \frac{1}{\lambda_k^{(2)}} \right)^{n-3} \frac{1}{(\lambda_l^{(3)})^2} \\ &+ \dots + \left(\frac{1}{\lambda_i^{(1)}} + \frac{1}{\lambda_k^{(2)}} \right)^2 \frac{1}{(\lambda_l^{(3)})^{n-3}} \\ &\left. + \left(\frac{1}{\lambda_i^{(1)}} + \frac{1}{\lambda_k^{(2)}} \right) \frac{1}{(\lambda_l^{(3)})^{n-2}} \right\}. \end{aligned} \quad (78)$$

In order to find the non-zero terms with the lowest order of $\frac{1}{(\lambda_q^{(m)})}$, $q = (i, k, l)$, we apply (69) and (73) to (78). This means that when $L_1 = L_2 = L_{12}$, the non-zero terms with the lowest order of $\frac{1}{(\lambda_q^{(m)})}$, $q = (i, k, l)$ are contained in

$$t_d(n) = \left(\frac{1}{\lambda_i^{(1)}} + \frac{1}{\lambda_k^{(2)}} \right)^{n-L_3} \frac{1}{(\lambda_l^{(3)})^{L_3-1}}, \quad n - L_3 = L_{12} \quad (79)$$

whereas, for $L_1 \neq L_2$, such terms are contained in $t_d(n)$ corresponding to two different values of n . In particular, these values are $n_1 = L_1 + L_3$ and $n_2 = L_2 + L_3$. Furthermore, applying (69), $t_d(n)$ reduces to

$$\begin{aligned} t_d(n) &= \left(\frac{1}{(\lambda_i^{(1)})^{n-L_3-1}} + \frac{1}{(\lambda_k^{(2)})^{n-L_3-1}} \right) \frac{1}{(\lambda_l^{(3)})^{L_3-1}} \\ t_d(n_1) &= \frac{1}{(\lambda_i^{(1)})^{L_1-1}} \frac{1}{(\lambda_l^{(3)})^{L_3-1}}, \\ t_d(n_2) &= \frac{1}{(\lambda_k^{(2)})^{L_2-1}} \frac{1}{(\lambda_l^{(3)})^{L_3-1}}. \end{aligned} \quad (80)$$

Applying (80) in (78), $P_{o,fr}$ is approximated at high SNR as

$$\begin{aligned} P_{o,fr} &\approx \frac{\tilde{r}_1^{L_1+L_3}}{(L_1+L_3)!} \sum_{i=1}^{L_1} \frac{a_i^{(1)}}{(\lambda_i^{(1)})^{L_1-1}} \sum_{l=1}^{L_3} \frac{a_l^{(3)}}{(\lambda_l^{(3)})^{L_3-1}} \\ &+ \frac{\tilde{r}_1^{L_2+L_3}}{(L_2+L_3)!} \sum_{k=1}^{L_2} \frac{a_k^{(2)}}{(\lambda_k^{(2)})^{L_2-1}} \sum_{l=1}^{L_3} \frac{a_l^{(3)}}{(\lambda_l^{(3)})^{L_3-1}}. \end{aligned} \quad (81)$$

Applying (69) in (81), $P_{o,fr}$ is further expressed as

$$\begin{aligned} P_{o,fr} &\approx \frac{\tilde{r}_1^{L_1+L_3}}{(L_1+L_3)!} \frac{1}{\prod_{i=1}^2 \lambda_i^{(1)} \prod_{l=1}^2 \lambda_l^{(3)}} \\ &+ \frac{\tilde{r}_1^{L_2+L_3}}{(L_2+L_3)!} \frac{1}{\prod_{k=1}^2 \lambda_k^{(2)} \prod_{l=1}^2 \lambda_l^{(3)}} \end{aligned} \quad (82)$$

which means that $P_{o,fr}$ is generalized as in (40). This completes the proof of the Proposition 4. \square

REFERENCES

- [1] J. Lee, M. Rim, and K. Kim, "On the outage performance of selection amplify-and-forward relaying scheme," *IEEE Commun. Lett.*, vol. 18, no. 3, pp. 423-426, Mar. 2014.
- [2] Y. G. Kim and N. C. Beaulieu, "Exact BEP of decode-and-forward cooperative systems with multiple relays in Rayleigh fading channels," *IEEE Trans. Veh. Technol.*, vol. 64, no. 2, pp. 823 - 828, Feb. 2015.
- [3] M. K. Arti and M. R. Bhatnagar, "Maximal ratio transmission in AF MIMO relay systems over Nakagami- m fading channels," *IEEE Trans. Veh. Technol.*, vol. 64, no. 5, pp. 1895 - 1903, May 2015.
- [4] B. Wang, J. Zhang, and A. Host-Madsen, "On the capacity of MIMO relay channels," *IEEE Trans. Inf. Theory*, vol. 51, no. 1, pp. 29-43, Jan. 2005.
- [5] C.-X. Wang, F. Haider, X. Gao, and et al, "Cellular architecture and key technologies for 5G wireless communication networks," *IEEE Commun. Magazine*, vol. 52, no. 2, pp. 122-130, Feb. 2014.
- [6] V. Tarokh, H. Jafarkhani, and A. R. Calderbank, "Space-time block codes from orthogonal designs," *IEEE Trans. Inf. Theory*, vol. 45, no. 5, pp. 1456-1467, July 1999.
- [7] M. Gharavi-Alkhansari and A. B. Gershman, "Constellation space invariance of orthogonal space-time block codes," *IEEE Trans. Info. Theory*, vol. 51, no. 1, pp. 331-334, Jan. 2005.
- [8] B. K. Chalise and A. Czylik, "Exact outage probability analysis for a multiuser MIMO wireless communication system with spacetime block coding," *IEEE Trans. Veh. Technol.*, vol. 57, no. 3, pp. 1502-1512, May 2008.
- [9] Third Generation Partnership Project, "Evolved universal terrestrial radio access (E-UTRA); Physical channels and modulation," *3GPP TS 36.211*, version 9.0.0, Release 9.
- [10] P. Dharmawansa, M. R. McKay, and R. K. Mallik, "Analytical performance of amplify-and-forward MIMO relaying with orthogonal space-time block codes," *IEEE Trans. Commun.*, vol. 58, no. 7, pp. 2147- 2158, July 2010.

- [11] Y. Dhungana, N. Rajatheva, and C. Tellambura, "Dual hop MIMO OSTBC for LMS communication," *IEEE Commun. Lett.*, vol. 1, no. 2, pp. 105-108, Apr. 2012.
- [12] T. Q. Duong, G. C. Alexandropoulos, H.-J. Zepernick, and T. A. Tsiftsis, "Orthogonal space-time block codes with CSI-assisted amplify-and-forward relaying in correlated Nakagami- m fading channels," *IEEE Trans. Veh. Technol.*, vol. 60, no. 30, pp. 882-889, Mar. 2010.
- [13] K. Yang, J. Yang, and L. Cai, "Dual-hop MIMO relaying with OSTBC over doubly-correlated Nakagami- m fading channels," *Eurasip Jr. Wireless Commun. Netw.*, 2012, 2012:294.
- [14] B. K. Chalise and L. Vandendorpe, "Outage probability analysis of a MIMO relay channel with orthogonal space-time block codes," *IEEE Commun. Lett.*, vol. 12, no. 4, pp. 280-282, Apr. 2008.
- [15] L. Yang and Q. T. Zhang, "Performance analysis of MIMO relay wireless networks with orthogonal space-time block codes," *IEEE Trans. Veh. Technol.*, vol. 59, no. 7, pp. 3668-3674, Sep. 2010.
- [16] L. Yang, M.-S. Alouini, K. Qaraqe, and W. Liu, "On the performance of dual-hop systems with multiple antennas: effects of spatial correlation, keyhole, and co-channel interference," *IEEE Trans. Commun.*, vol. 60, no. 12, pp. 3541-3547, Dec. 2012.
- [17] M. L. Morris and M. A. Jensen, "Improved network analysis of coupled antenna diversity performance," *IEEE Trans. Wireless Commun.*, vol. 4, no. 4, pp. 1928-1934, July 2005.
- [18] C. P. Domizioli, B. L. Hughes, K. G. Gard, and G. Lazzi, "Receive diversity revisited: correlation, coupling and noise," in Proc. *IEEE GLOBECOM'07*, Washington, DC, Nov. 2007, pp. 3601-3606.
- [19] S. Krusevac, P. Rapajic, and R. A. Kennedy, "Channel capacity estimation for MIMO systems with correlated noise," in Proc. *IEEE GLOBECOM'05*, St. Louis, Nov.-Dec., 2005, pp. 2812-2816.
- [20] Y. Dong, C. P. Domizioli, and B. L. Hughes, "Effects of mutual coupling and noise correlation on downlink coordinated beamforming with limited feedback," *EURASIP Jm. Adv. Signal Process.*, vol. 2009, Article ID 807830.
- [21] K. S. Gomadam and S. A. Jafar, "The effect of noise correlation in amplify-and-forward relay networks," *IEEE Trans. Inf. Theory*, vol. 55, no. 2, pp. 731-745, Feb. 2009.
- [22] Y. Hassan, R. T. L. Rolny, and A. Wittneben, "MIMO relaying with compact antenna arrays: coupling, noise correlation and superdirectivity," *IEEE 24th PIMRC*, London, UK, Sept. 2013, pp. 1070 - 1076.
- [23] B. Chalise, Y. Zhang, and M. Amin, "Local CSI based selection beamforming for AF MIMO relay system with direct link," *IEEE Commun. Lett.*, vol. 16, no. 5, pp. 622-625, May 2012.
- [24] K. B. Petersen and M. S. Pedersen, *Matrix cookbook*, Available online at www.imm.dtu.dk.
- [25] L. Han, J. Mu, W. Wang, and B. Zhan, "Optimization of relay placement and power allocation for decode-and-forward cooperative relaying over correlated shadowed fading channels," *Eurasip Jr. Wireless Commun. Netw.*, 2014, 2014:41.
- [26] S. Shahbazpanahi, M. Beheshti, A.B. Gershman, M. Gharavi-Alkhansari, and K.M. Wong, "Minimum variance linear receivers for multiaccess MIMO wireless systems with space-time block coding," *IEEE Trans. Signal Process.*, vol. 52, pp. 3306-3313, Dec. 2004.
- [27] M. Chiani, M. Z. Win, and A. Zanella, "On the capacity of spatially correlated MIMO Rayleigh fading channels," *IEEE Trans. Inf. Theory*, vol. 49, no. 10, pp. 2363-2371, Oct. 2003.
- [28] D. R. Cox, *Renewal Theory*, London: Methuens Monographs on Applied Probability and Statistics, 1967.
- [29] M. Bengtsson and B. Ottersten, "Optimum and suboptimum transmit beamforming," *Handbook of Antennas in Wireless Communications*, CRC Press, 2002.
- [30] I. S. Gradshteyn and I. M. Ryzhik, *Table of Integrals, Series, and Products*, A. Jeffrey, ed., sixth edition. Academic Press, 2000.
- [31] J.-B. Kim, D. Kim, "Comparison of tightly power-constrained performances for opportunistic amplify-and-forward relaying with partial or full channel information," *IEEE Commun. Lett.*, vol. 13, no. 2, pp. 100-102, Feb. 2009.
- [32] B. K. Chalise, W.-K. Ma, Y. D. Zhang, H. A. Suraweera, and M. G. Amin, "Optimum performance boundaries of OSTBC based AF-MIMO relay system with energy harvesting receiver," *IEEE Trans. Signal Process.*, vol. 61, no. 17, pp. 4199-4213, Sep. 2013.
- [33] M. K. Simon and M.-S. Alouini, *Digital communication over fading channels*, John Wiley & Sons, 2005.
- [34] H. Cramèr, *Random variables and probability distributions*, Cambridge, UK: Cambridge University Press, 1970.